ANALYSES ON TRANSIENT HEAT TRANSFER FROM ANOMALOUS SHAPES WITH HETEROGENEOUS PROPERTIES

By

RALPH EDWARD SMITH

Bachelor of Science in
Agricultural Engineering
University of Georgia
Athens, Georgia
1948

Master of Science
University of Georgia
Athens, Georgia
1961

Submitted to the faculty of the Graduate
College of the Oklahoma State University
in partial fulfillment of the
requirements for the degree
of
DOCTOR OF PHILOSOPHY
May, 1966

ANALYSES ON TRANSIENT HEAT TRANSFER FROM ANOMALOUS SHAPES WITH HETEROGENEOUS PROPERTIES

Thesis Approved:

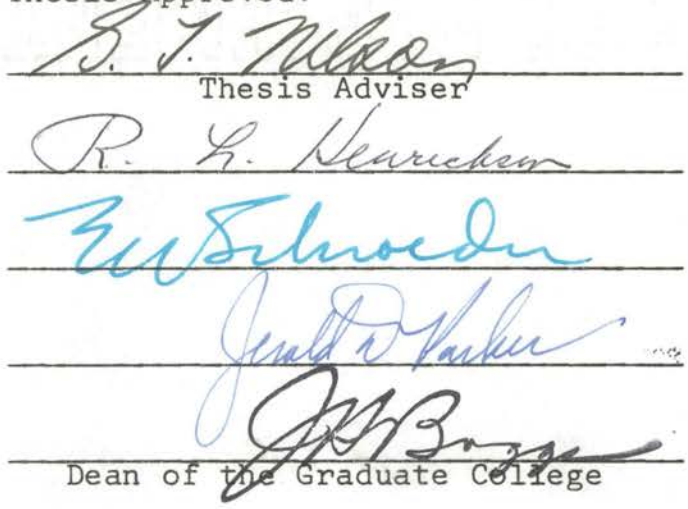

Thesis Adviser

Dean of the Graduate College

PREFACE

This investigation was conducted as a part of the Oklahoma Agricultural Experiment Station Project 1268. The project has been financed in part by the Transportation and Facilities Research Division, ARS, USDA.

Research was initiated in June, 1963, under the supervision of Dr. R. L. Henrickson, Professor of Animal Science, to determine the feasibility of processing the pork carcass prior to chilling. The work progressed to the development of "in-the-line" processing methods and procedures for the "hot pork" carcass. The Agricultural Engineering Department began cooperating with the Animal Science Department to design a cooling cabinet for the rapid cooling of the various commercial cuts of pork. The need for basic heat transfer information for these anomalous shapes provided the stimulus for accomplishing the research reported in this thesis.

I wish to express sincere appreciation to Dr. G. L. Nelson, who served as Major Adviser for my graduate study. He has been a source of real assistance, inspiration, and encouragement.

Appreciation is extended to other members of the Advisory Committee. Professor E. W. Schroeder, Head of

the Agricultural Engineering Department, Dr. J. D. Parker, Professor of Mechanical Engineering, and Dr. R. L. Henrickson, Professor of Animal Science served in this capacity. Their aid and encouragement have been invaluable.

A special word of thanks is extended to Professor Schroeder for his efforts in his role as administrative supervisor of the graduate program. Appreciation is extended to him and the National Science Foundation for providing the Graduate Traineeship during the period of the graduate study.

During the conduct of the study there were many colleagues in research in the Departments of Agricultural Engineering and Animal Science who gave assistance and encouragement. My appreciation is extended to these. I acknowledge with appreciation the assistance given by Dr. J. E. Garton, Professor of Agricultural Engineering, in the design of the nomograph used in the study. And for the preparation of the figures, acknowledgment of appreciation is extended to Mr. Jack Fryrear and to Mr. Don McCrackin.

For their many sacrifices and cheerful deferences to the task I dedicate this thesis to my wife Carolyn and my children, Susan, Ellen, and Edward.

TABLE OF CONTENTS

LIST OF TABLES

LIST OF FIGURES

CHAPTER I

INTRODUCTION

The Problem

Research on the processing of pork products prior to chilling brought attention to the difficulties in quantitatively predicting transient heat transfer relationships involved with anomalous shapes. Values of the thermal properties for meat products, and agricultural products in general, are not well known and because of the nature of the materials are difficult to evaluate. Besides the characteristic anomalous shapes encountered with the pork products the different cuts are generally heterogeneous in composition. Also with meat products there is the additional difficulty of anisotropy of thermal conductance with respect to the fiber direction. Consequently, there is a need for the evaluation of thermal diffusivity and other thermal properties for various meat cuts in the shapes in which they occur. Techniques developed for evaluating the thermal properties for meat products will be valuable for such measurements for other agricultural products.

The ability to evaluate object geometry will make it possible to determine thermal properties and will prove

valuable in the development of prediction equations and graphical solutions for the transient heat flow for anomalous shapes. Design applications involving transient conduction heat transfer from such shapes in the past have resorted to costly design by adaptation and overdesign. No one has adequately dealt with this geometry problem. The anomalous shape has commonly been replaced by a regular shape, for which a solution exists, that is arbitrarily determined best replaces the shape. While geometry analysis for anomalous shapes inevitably will be an approximation technique it offers a rationally derived general solution for the infinite geometries that exist.

Objectives

The objectives of this study were as follows:

1. To derive a model to represent anomalous shapes during transient heat exchange.

2. To define a parameter G to serve as an index of geometry for different shapes.

3. To develop a prediction equation for values of G to be calculated from dimensions taken from the anomalous shape.

4. To conduct experiments to test the validity of the prediction equation to predict values of G for the geometrical model and for anomalous shapes.

5. To demonstrate the use of geometry analysis to

measure "effective" values of thermal diffusivity, thermal conductivity, and surface conductance for different cuts of pork.

6. To relate the location of the mass-average temperature of an object to its characteristic length.

Assumptions and Limitations

The analytical developments of prediction equations for transient conduction heat transfer usually are based on the assumptions of a constant initial temperature throughout the object and the maintenance of a uniform temperature over the surface during the period of transient exchange. These conditions are difficult or impossible to attain under practical circumstances. Considerable effort was expended in all the tests to attain the conditions and the results were treated as though they were attained. When the test material was obviously heterogeneous and anisotropic in physical and chemical properties the values of the thermal properties measured are assumed to be "effective" or average values.

Definition of Symbols

The symbols used in this report are generally the same as ones finding common usage in the literature of heat transfer. Unfortunately, there is not an approach to a unanimity of usage in the literature on any of the quantities described.

The dimensionless parameters denoted by the letters Bi and Fo provide a means of recognition to Biot and Fourier for their roles in developing these important dimensionless parameters and are never confused with the products of quantities B × i and F × o. A practice was followed, with one exception, in employing the lower case letter to represent a variable quantity and the upper case letter as a ratio involving the quantity, e.g., t is used for temperature and T for a temperature ratio. The exception was the use of m to represent the reciprocal of the Biot number. This follows the practice of Heisler (13) who developed the most widely used graphical solutions of transient heat transfer for the regular geometrical shapes. The definitions of symbols are made at the point where they are introduced in the report.

CHAPTER II

REVIEW OF THE LITERATURE

Introduction

The literature comprising the theoretical basis of transient heat transfer is very large. This problem has served as the vehicle for the development of many of the most sophisticated mathematical tools since the great success of Fourier. However, the complex solutions were put to little practical use for fully a hundred years after the developments of Fourier until the introduction of a new approach to the problem early in this century. The new development was done by engineers and engineering-oriented mathematicians and scientists employed by industry. It followed the intensive development of the principles of similitude in the second and third decades of this century by men such as Buckingham, Rayleigh, and Bridgman.

Conceptual Development

The basic analyses presented by Fourier (8) in 1822 continue to form the foundation of the analytical solutions for transient heat flow from solids. Mathematical analysis is greatly enriched by the concepts and techniques that he

devised to deal with the heat conduction problem. Spanning a hundred years, physicists Williamson and Adams (28) modestly presented a paper relating to their work in applying heat transfer to glass manufacture. Material from this paper giving solutions for most of the regular geometrical shapes is widely used in the literature. The new era for the development of transient heat transfer from solids can be traced to this report. Three ideas that have been important in the conceptual development are listed here.

1. "The similarity of the equations . . ." The form of the equations for different geometries is basically similar.

2. "At all save the shortest times it is only necessary to use one term of the series . . ." A plot of time versus the logarithm of temperature is a linear plot except for the earliest period of time.

3. "The more involved [cases] are products of the less involved . . ." An example of this idea is to predict the temperature at a point in a finite cylinder from the product of temperature ratios for the point in an infinite cylinder and an infinite slab. We may note the role of the three mutually orthogonal dimensions in applying the concept of the product solution. The implication of a product solution for an exponential relationship such as this is that a factor from the resultant exponent is formed as a summation of independent components of the original exponents.

The first graphical solutions of transient conduction heat transfer problems were presented in 1923 by Gurney and Lurie (10). Following closely the intensive development of the principles of similitude by Buckingham (3) and others in this field, they presented their graphical solutions with the explanation:

> The [solutions] were obtained by converting some of the more common formulas for heat diffusion into expressions containing pure ratios or nondimensional variables only, thereby enormously reducing the necessary basic calculations as well as extending the field of applicability.

The solutions left something to be desired in accuracy of readings and ease of use. They represent a significant advancement conceptually. They made possible a practical use of the prediction equations for transient heat transfer from the basic geometrical shapes. An especially revealing comment of Gurney and Lurie on the use of the analytical solutions is their remark, 100 years after Fourier's work, that their solutions "may help to realize Fourier's wish . . . that his mathematics be applied to industry."

Graphical solutions have come to be an accepted method of solution for transient conduction heat transfer problems. The chief limitation often is in fitting the geometry of the object of interest to the proper time-temperature chart. Other difficulties are related to uncertainty concerning thermal properties of the object and adherence to the

assumptions on which the charts are based. The most complete and useful charts to date are the ones prepared by Heisler (13).

The presentation of analytical solutions in recent heat transfer texts are often in such a way as to emphasize the similarity of form of equations for the different geometrical shapes, e.g., Schneider (24). It is universally acknowledged that for practical use the time-temperature history for a point within an object during transient heat exchange, except for a brief initial time period, is accurately described by the first term of the appropriate series solution. Heisler (13) has a strong discussion in his paper regarding this point. Inspection of his time-temperature charts reveals essentially straight line plots of distributions of the Fourier number, a dimensionless time index, versus the logarithm of the temperature ratio at the center of the different objects for values of the Fourier number of 0.2 and greater.

A recent theoretical development derived general expressions for unsteady temperature distributions in finite regions of arbitrary geometry (20). The mathematical description of a specific geometry is introduced into the general solution to obtain the usual infinite series solution. The implication may be inferred that if the geometry of an anomalous shape could be mathematically described then the complete solution could be obtained for the

particular shape. While such a procedure is not technically feasible for all except the regular shapes, the idea is useful to indicate what might be done on the basis of a heat transfer equation simplified to one term.

Analytical Development

The analytical derivations of the transient conduction heat transfer equations for the regular geometrical shapes are, as noted, based upon the work of Fourier. Only recently have investigators begun to apply the analytical methods to the problems of heat flow from shapes other than the basic shapes. High-speed computers are employed for the solutions of these more complex problems. And, it might be noted that the services of a computer are required when answers are sought for a problem with specified conditions.

A recent paper by Kirkpatrick and Stokey (16) illustrates the use of computers in solving the highly complex problem. They present the solution for the transient heat conduction from infinitely long elliptical cylinders for four values of eccentricity for the elliptical cross section. They present tabular solutions for 30 selected points and four values of the Fourier number and give temperature distributions for the center points of the four cylinders. Their work points to the fact that practical use may be made of

tabular solutions and graphs of temperature distributions rather than the complex equations derived.

The capability of the high-speed computer is directed toward the solution of another complex problem that has resisted solution by hand computation in the work of Haji-Sheikh (11). The geometrical shape is the prolate spheroid and the boundary condition of negligible surface thermal resistance is assumed. Temperature distributions are given for the center and focus points for six values of the ratio of major to minor axes. Tables are given for evaluating the eigenvalues and constants of the doubly infinite series solution. The computer is required to apply the information to specified problems and solutions are for the six specified ellipsoids arbitrarily selected from an infinite number of different geometrical shapes existing as eccentricity ranges from zero for a sphere to one for an infinite cylinder. Information from these solutions may be used as checkpoints in comparison with a simplified solution using one term of the infinite series and values of the eigenvalues for ellipsoids are predicted by an approximation technique.

Evaluation of Thermal Properties

It is difficult to trace the origin of the idea of using time-temperature data from a specified geometrical shape during transient heat exchange to measure thermal

diffusivity. The thought is so basic to the derived heat conduction equation that its origin might be attributed to Fourier. Several reports early in this century note that such a procedure may be followed (4, 14, 26). In the case of each report of experimental work the test shapes were regular geometrical shapes or they were considered to approximate a regular shape.

Much early work done in this area was by investigators in the field of food science. Their work was primarily with food products in cylindrical cans. The earliest report of values of thermal diffusivity are in the report by Thompson (26). The reports of these early food scientists were reviewed at length in 1942 by Olson and Jackson (21) and more recently by Ball and Olson (1). A method is described for evaluating thermal diffusivity for specific geometries by means of a time parameter which indicates the measure of time required for the original temperature difference of object and environment to be changed by one logarithm cycle. The methods and symbols of this particular school of investigators appear to have widespread acceptance in the food processing industry.

In a recent report by Dickerson (6) an apparatus is described for measuring thermal diffusivity with transient heat exchange data. The test material, in liquid or granular form, is placed in a cylindrical container to establish the geometrical configuration. Diffusivity is determined by

means of an analytical development relating the axial and surface temperatures of test material. A steady temperature difference is reached during heating or cooling of the product in a water bath whose temperature increases or decreases linearly in time. Accuracy of about 5 per cent is claimed for his apparatus.

Time-temperature data during transient heat exchange has been used to evaluate the thermal properties of fruits and vegetables, e.g., Bennett (2), Gane (9), and Perry, et al. (23). Experimental material was considered to approximate the regular geometrical shapes in each of these examples. However, in the work reported by Perry, et al. a geometry correction was introduced "by observing cooling rates of cast aluminum models of citrus fruits." The authors did not explicitly represent this as a geometry correction, but such a correction is combined with their stated purpose to correct for surface thermal resistance. To assume that the anomalous shapes of practically any agricultural products will approximate the regular geometries of the sphere, cylinder, or slab will introduce some undeterminable error in evaluated thermal properties.

Experimental information was presented recently to show that for spherically shaped peaches the mass-average temperature remains at a fixed point on the characteristic length during transient cooling (24). From this report a mass-average temperature is defined as a temperature that

"denotes a single value from the temperature distribution that would become the uniform [object] temperature under adiabatic conditions". Carslaw and Jaeger (5) have curves from theoretical calculations giving values of the mass-average temperature in time for the sphere, infinite cylinder, and infinite slab. Transferring values of the mass-average temperature to charts of temperature distributions for the three shapes for various values of time shows that for a particular geometry the location of mass-average temperature does remain stable in its location during the transient period. It appears that the location of the mass-average temperature might be related to the object geometry. A difficulty in measuring the precise value of the temperature is that the temperature gradient is steepest for this portion of the temperature distribution.

Some form of the method of the "guarded hot-plate" is usually employed to measure thermal conductivity. Three recent reports using this method indicate values of conductivity for various meat products (17, 18, 27). This problem is made difficult to solve by the nature of the material: heterogeneity; variations in the proportions of lean, fat, bone, and water content; variation in the properties of a single component such as the fat; and anisotropy of the thermal conductivity. Such problems help to explain why there is a disconcerting variance in values of thermal properties that one may find by consulting different sources of tables of published values.

CHAPTER III

THEORETICAL ANALYSIS

Introduction

It would seem highly desirable to have an approximation procedure that is simple to use and, commensurate with the input data, accurate to predict heat conduction relationships for the vast number of cases where the object geometry is not readily defined. The procedure might find favor for use when object geometry is defined if a considerable saving in time is effected in comparison with the use of the infinite series solutions of exponential and trigonometric product terms. In spite of all the methods for evaluating thermal properties very little information is available for materials such as the many agricultural products. Solution of the geometry problem might facilitate the evaluation of "effective" thermal properties of heterogeneous products whose values are inextricably related to characteristic anomalous shapes.

The Model

For the purpose of describing the temperature at a point in an anomalous shape during transient heat transfer

the general ellipsoid is proposed to serve as an adequate model of the actual object. Justification for the selection of this model, that is considered most feasible, will be given later. That the general ellipsoid is not easily formed with tools that are generally available does not represent a crucial difficulty since the use of the model is essentially conceptual. When a physical model is required ellipsoids of revolution, the prolate and oblate spheroids, serve as special cases of the general ellipsoid. A broad range of anomalous shapes are envisioned, but some obvious restrictions and adaptations are required.

The ellipsoidal model and anomalous shape are related in that the minimum semi-thickness through the center-of-mass defines the characteristic length ℓ for both the model and the shape (Figure 1). The basic objective in defining the characteristic length is to indicate the minimum distance across which the maximum temperature difference exists during the transient period. Orthogonal cross-sections containing ℓ are taken from the anomalous shape that are generally the smaller and larger cross-sections in planes of ℓ. The areas are replaced by ellipses of the same cross-sectional area that define the ellipsoidal model. Values of a and b, semi-major axes of the ellipses, are not obtained by measurement from the object cross-sections but are easily calculated. The areas of the ellipses are $\pi\ell a$ and $\pi\ell b$ which are equated to the orthogonal

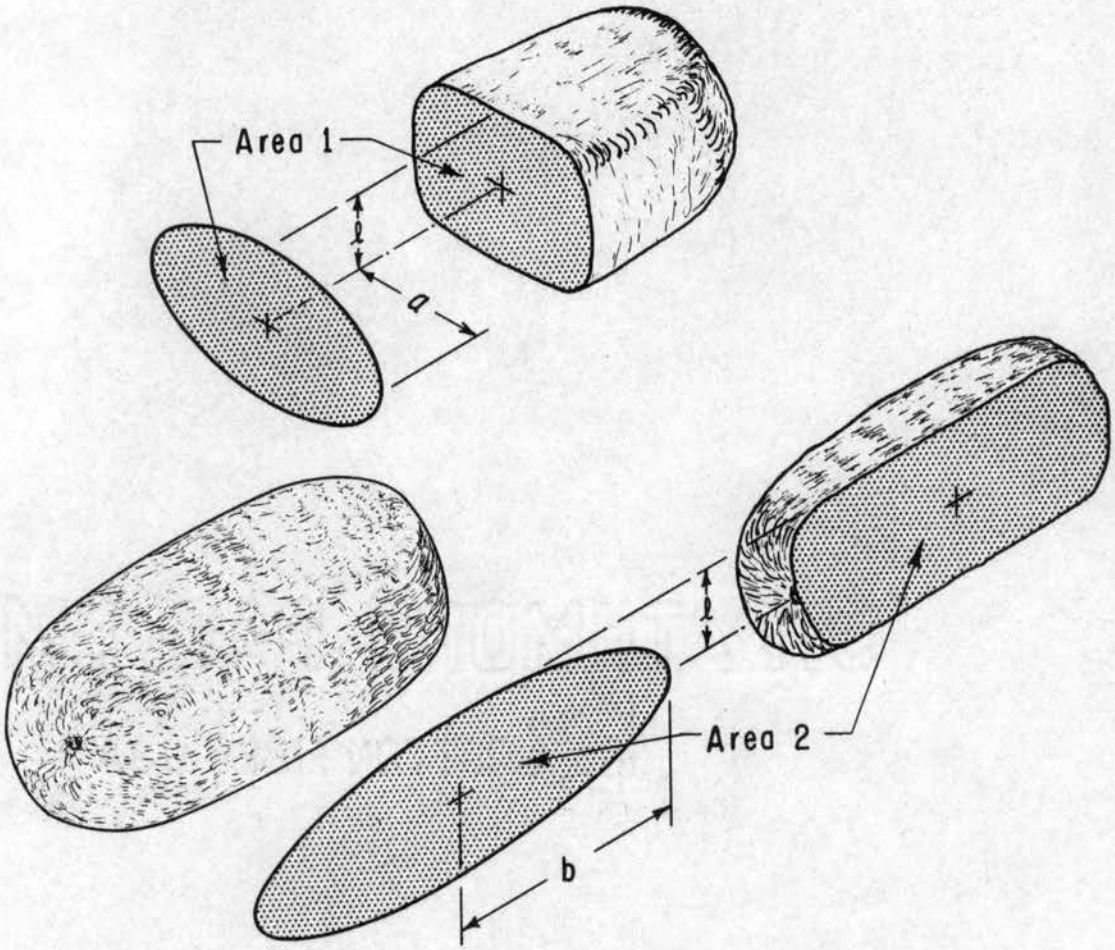

Figure 1. A boneless processed ham as an anomalous shape is replaced by an ellipsoidal model

areas from the anomalous shape. Thus we have the following distance ratios:

$$\frac{a}{\ell} = \frac{\text{Area 1}}{\pi \ell^2} \text{ and } \frac{b}{\ell} = \frac{\text{Area 2}}{\pi \ell^2}$$

These dimensionless distance ratios are defined as A and B, respectively, and are used to describe the object geometry.

The analysis of different anomalous shapes will call for different adaptive procedures for replacing a shape with its ellipsoidal model. Validity of the results are enhanced if the anomalous shapes have some measure of regularity. Instead of allowing repitition of a significant portion of the isothermal shells, the shape can be divided into two anomalous shapes. An example of this is the commercial pork cut known as the loin strip. This cut is about two feet long with a rather characteristic cross-section in the shape of a pork chop. The shape is more massive at the ends with a narrowing in the middle. To study the thermal properties of this shape it may be divided into two anomalous shapes.

An idealized half-section of a loin strip was constructed from acrylic plastic and is shown in Figure 2 to further illustrate the application of the ellipsoidal model to replace an anomalous shape. A geometrically similar pork chop cross-section is maintained over a 12 inch length with a linearly changing area. An analogic experiment was conducted to locate the point in Area 1 whose

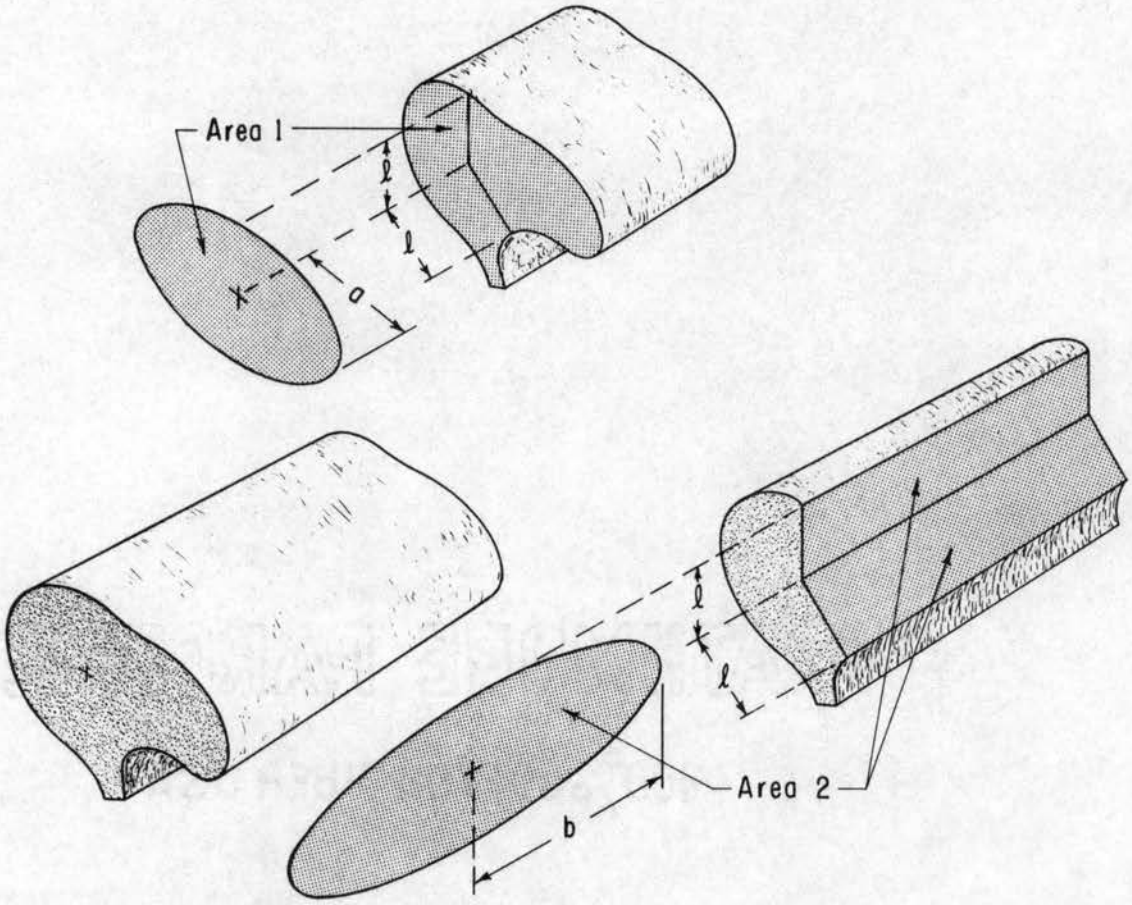

Figure 2. A plastic model of a pork loin strip as an anomalous shape replaced by an ellipsoidal model

temperature during transient heat exchange gives the maximum temperature difference when compared to the surface temperature. Characteristic length is seen as the path from this point to the nearest surface. This leads to an offset cut to obtain the orthogonal Area 2. Such a careful analysis is not possible with the actual pork cut; the general procedure, however, may be followed for such cases.

The usual boundary conditions regarding temperatures are assumed. The object, initially at a uniform temperature t_i, is suddenly removed (at $\tau = 0$) to an environment at a different temperature t_o that is maintained during the transient period of heat exchange. The environment is assumed to produce a convective heat exchange at the surface of the object. If large values of temperature difference occur between the surface and environment, it will lead to significant radiative exchange that may be calculated and subtracted from the convective component of heat exchange. Temperatures of interest in the object are restricted by this analysis to points along the characteristic length. This provides a sample of all temperatures existing within the object during the period of transient exchange.

Methods of Similitude

After the manner of Gurney and Lurie (10) who first applied the methods of similitude to the solution of the

transient conduction heat transfer problem, the following analysis is given with two dimensionless groups added for describing object geometry. Their analysis, and the subsequent presentations of others, account for object geometry by restricting the analysis to a specific geometry.

The following pertinent quantities are listed:

1. $\Delta t_i = t_i - t_o$, initial temperature difference between object temperature t_i and environment temperature t_o, °F
2. $\Delta t_d = t_d - t_o$, temperature difference at a specified time τ between the temperature t_d at point d and the environment temperature t_o, °F
3. k, object thermal conductivity, Btu/hr °F ft
4. c_p, object specific heat, Btu/lb °F
5. h, object surface conductance, Btu/hr °F ft^2
6. ρ, object density, lbs/ft^3
7. τ, elapsed time, hr
8. ℓ, characteristic length or minimum distance within the object with maximum temperature difference during transient period, ft
9. a, semi-major axis of smaller model ellipse, ft
10. b, semi-major axis of larger model ellipse, ft
11. ℓ_d, distance to a point on ℓ from object center, ft

By the Buckingham Pi Theorem 11 quantities minus 5 dimensions gives 6 dimensionless groups to be formed. In

the second Pi term the quantity α, thermal diffusivity, is defined as $k/\rho c_p$ with units of ft^2/hr. They are listed with associated familiar heat transfer symbols:

Pi term	Parameter	Symbol
1. $\frac{\Delta t_i}{\Delta t_d}$	Temperature ratio	T
2. $\frac{\alpha\tau}{\ell^2}$	Fourier number	Fo
3. $\frac{h\ell}{k}$	Biot number	Bi
4. ℓ_d/ℓ	Distance ratio	L_d
5. a/ℓ	Distance ratio	A
6. b/ℓ	Distance ratio	B

The temperature ratio T denotes the existing temperature ratio at a point d for a specified time. The Fourier number is a time index. It measures the degree to which heating or cooling effects have penetrated the object. The Biot number indicates the ratio of resistance to heat transfer at the surface to the internal heat resistance. The distance ratio L_d indicates the fractional distance from the center along the characteristic length where a temperature is located. The distance ratios A and B are used to define the geometry of the ellipsoidal model for the shape.

Development of Equations

The general form of the prediction equation is:

$$T = f_1(Fo,Bi,L_d,A,B) \qquad (1)$$

Derivations of the transient conduction heat transfer equations usually begin with a specified geometry. The geometry guides in the selection of an appropriate coordinate system and the method of obtaining the solution. For each geometry the goal is to find a solution to the Fourier Conduction Equation:

$$\frac{\partial T}{\partial \tau} = \alpha \nabla^2 T \tag{2}$$

Presentations of solutions for the regular geometrical shapes are found in many sources. A series solution for the parallelopiped that employs multiple Fourier series is given in Carslaw and Jaeger (5). The form of the solution for the boundary conditions of finite internal and surface thermal resistance, p. 184, makes use of the method of product solutions. Using the symbols of this report and with semi-thicknesses s_1, s_2, and s_3 (s_1 is characteristic length) the form of the solution is expressed in the equation:

$$T = \Psi_1(x,s_1,Bi)\Psi_2(y,s_2,Bi)\Psi_3(z,s_3,Bi) \tag{3}$$

The same solution given by Carslaw and Jaeger is also presented by Schneider (24), p. 253, in terms of symbols and parameters contained in this report. The solution is as follows:

$$\Psi_1(x,s_1,Bi) = 4 \sum_{n=1}^{\infty} \left[\frac{\sin M_n}{2M_n + \sin 2M_n} \right] \times e^{-M_n^2 Fo} \cos M_n \frac{x}{s_1} \qquad (4)$$

and similarly for Ψ_2 and Ψ_3. Equation 4 is the series solution for the infinite slab where the coefficient M_n denotes the roots of the transcendental equation developed by Fourier (8),

$$M_n \tan M_n = Bi \qquad (5)$$

Schneider develops the series solutions also for the infinite cylinder and the sphere in terms of the parameter M_n evaluated by a transcendental equation appropriate to the object geometry. This procedure emphasizes the similarity of form of the solutions for the different geometries. Conceptually one might consider that transcendental equations exist for an infinite progression of geometries ranging from the sphere to the infinite slab.

Within a limitation of interest to temperatures that occur along the characteristic length and the hypothesis that geometry may be predicted from the parameters A and B, Equations 3 and 4 serve to demonstrate for the parallelopiped the relationship indicated by Equation 1. With the further restriction to one term of the infinite series and the use of M_n as a parameter for any specified geometry, we may represent Equations 3 and 4 in the general form,

$$T = f_2(A,B,Bi,L_d)e^{-Fo[f_3(A,B,Bi)]^2} \tag{6}$$

or

$$T \equiv C\, e^{-M_1^2 Fo} \tag{7}$$

A geometry index G is defined as the number that when multiplied with π^2 gives the appropriate value to the coefficient M_1^2, in Equation 7, for the geometry concerned and the conditions of negligible surface thermal resistance. Under these conditions the first roots of the appropriate transcendental equations take on limiting values that suggest this means of defining a geometry parameter. Values of the indices range from 0.25 to 1.00 for the infinite slab and the sphere respectively. The index for anomalous shapes will be described by means of the distance ratios A and B. For the noted conditions the relationships are expressed by the equations,

$$M_1^2 = G\pi^2 \tag{8}$$

and

$$G = f_4(A,B) \tag{9}$$

The geometry index G is defined for the conditions of negligible surface thermal resistance. For other conditions the functional relationship between M_1^2 and G is indicated in Equation 6 and may be expressed in the form,

$$M_1^2 = f_3(G,Bi) \tag{10}$$

The three regular geometries of the sphere, infinite cylinder, and the infinite slab were used to evaluate f_3. Equation 4 for the infinite slab and corresponding equations for the infinite cylinder and sphere gave the values of G of 0.25, 0.586, and 1.00. The transcendental equations for these geometries were solved with a computer for assumed discrete values of Bi to give values of M_1^2. (Solutions for these equations are given in the literature, but not in discrete values that correspond for the values of m for the different geometries [5,24].) A log-log plot of values of M_1^2 versus G yielded a family of straight lines for the separate values of Bi including the limiting case when $Bi \to \infty$. This information was used to construct the nomograph of Figure 3. Values of m for the reciprocal of Bi are used according to the style of Heisler (13).

For the conditions of negligible surface thermal resistance the exponent of the equation resulting from the product solution indicated by Equation 3 is as follows:

$$M_1^2 Fo = \left[\frac{1}{4s_1^2} + \frac{1}{4s_1^2} + \frac{1}{4s_1^2} \right] \pi^2 \alpha \tau \qquad (11)$$

And by rearranging obtain the following equation,

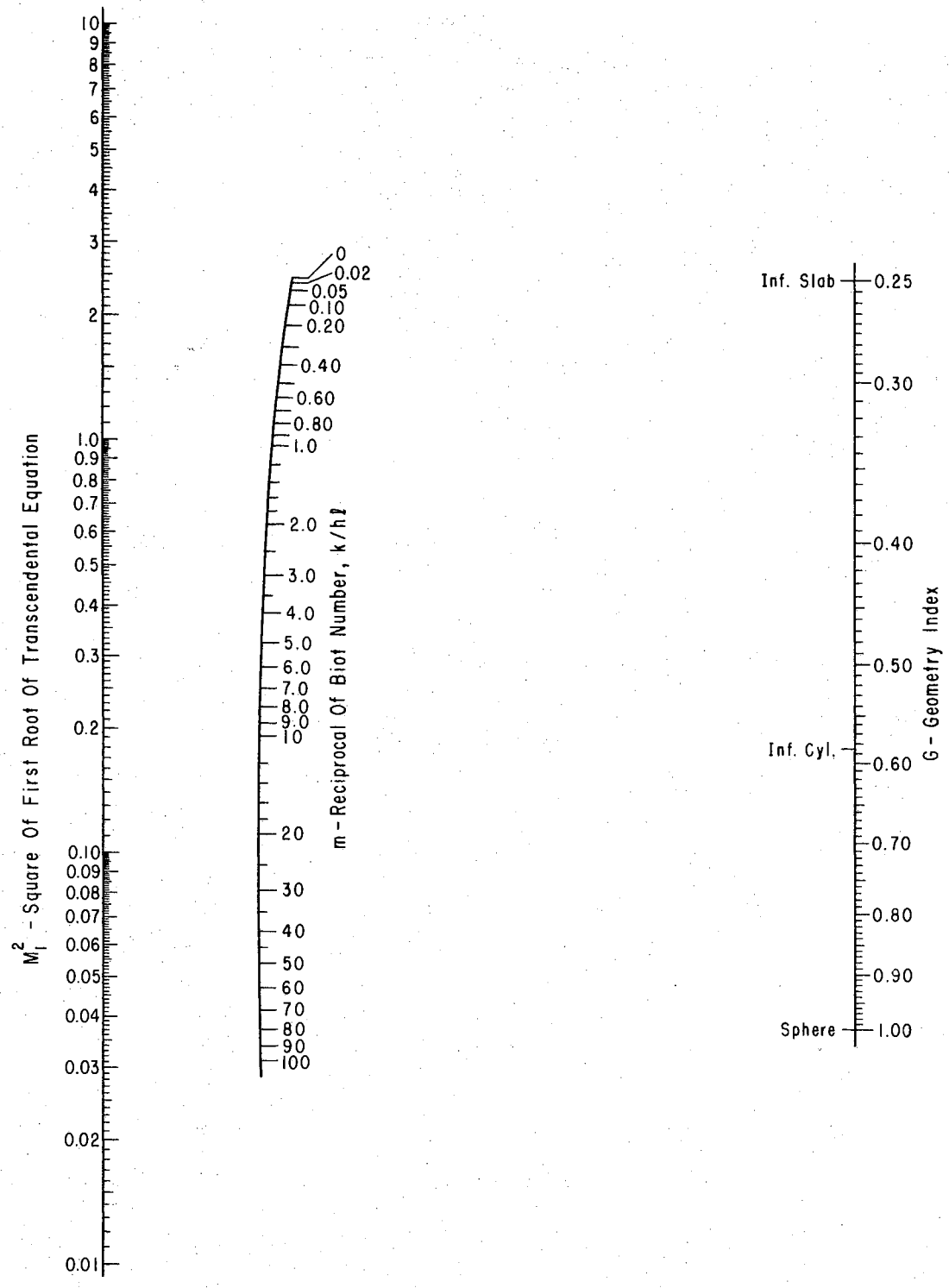

Figure 3. Nomograph for evaluating elements of the equation: $M_1^2 = f_3(G,Bi)$

$$M_1^2 Fo = \left[\frac{1}{4} + \frac{1}{4(s_2/s_1)^2} + \frac{1}{4(s_3/s_1)^2} \right] \pi^2 \frac{\alpha\tau}{s_1^2} \qquad (12)$$

Note that the bracketed quantity of Equation 12 takes on a specific fractional value for a brick whose dimensions are given. The manner of obtaining this index fits very well with the proposed concept of a geometry index G and two orthogonal distance ratios. But a parallelopiped model to replace anomalous shapes would generally be much less suitable than the ellipsoidal model. If we arbitrarily classify all finite shapes as ranging from a sphere to an infinite slab, the ellipsoidal model will adapt perfectly at the extremes to replace the shapes and it is hypothesized that it would adapt to other intermediate shapes with less distortion than any other model. The parallelopiped model would not fit for the sphere but would fit for the cube and other brick shapes extending to the infinite slab. Any randomly selected anomalous shape would be more adequately replaced by the ellipsoid than the parallelopiped. In all cases when the shape is a parallelopiped Equation 12 may be used to evaluate the geometry index G.

The analytical development of the equation for conduction heat flow from ellipsoids does not lead to a relationship such as Equation 12 for the parallelopiped. The work of Haji-Sheikh (11) may be used to obtain six values of M_1^2 for specific ellipsoids.

We may derive an equation for the ellipsoidal model by deductive reasoning in analogy with Equation 12. The results from this equation may be compared with the values from Haji-Sheikh's report and compared with experimental results. The following equation is deduced by analogy and the geometry indices of the sphere and infinite slab.

$$M_1^2 Fo = \left[\frac{1}{4} + \frac{3}{8A^2} + \frac{3}{8B^2}\right] \pi^2 \frac{\alpha\tau}{\ell^2} \tag{13}$$

Since the limiting cases of the ellipsoid are the sphere and the infinite slab it may be seen that the above equation gives the proper coefficients for these extreme cases, for the sphere when A=B=1 and for the infinite slab when A=B=∞. These limiting cases, when we assume the form analogous to Equation 12, are sufficient to establish the constants of the bracketed term as given. This term then gives us the required equation for relating geometry index G to the distance ratios A and B.

$$G = \frac{1}{4} + \frac{3}{8A^2} + \frac{3}{8B^2} \tag{14}$$

A comparison is made in Table I of the geometry index G from Equation 14 and the geometry index derived from the first eigenvalues of the doubly infinite series equation developed by Haji-Sheikh for the prolate spheroid. A check was also made by means of readings from temperature distributions given in his report for the different

spheroids for values of the Fourier number of 0.20 and 0.50 and calculating an average slope for the distribution by means of regression analysis. It depends upon how close one chooses to estimate readings from a graph, but the geometry indices obtained from the values are essentially the same as those predicted by Equation 14 except for the last spheroid with B=5.0. In this case there is a difference of about 6%. There is an explanation in his report of uncertainty about the distribution for this shape that is due to a word-length limitation of the computer.

TABLE I

GEOMETRY DATA FOR PROLATE SPHEROIDS

Distance A	Ratio B	Predicted Geometry Index G Ref. (11)	Predicted Geometry Index G Eqn. 14
1.00	1.10	0.942	0.935
1.00	1.20	0.898	0.885
1.00	1.50	0.810	0.792
1.00	2.00	0.739	0.719
1.00	3.00	0.679	0.667
1.00	5.00	0.638	0.640

Values of the geometry index G may be predicted with Equation 14 in those cases where the geometry is anomalous.

Equation 12 may be used when the geometry is that of a parallelopiped. In those cases where the geometry is a finite cylinder (length c and diameter d) geometry index may be calculated from an equation adapted from the report of Williamson and Adams (28) as follows:

$$G = 0.586 + \frac{1}{4(c/d)^2} \qquad (15)$$

Relationships for Mass-Average Temperatures

When a semi-log graph is constructed of mass-average temperature versus the Fourier number for the sphere and infinite slab and the linear portions of the plots for these geometries are extrapolated to a point of intersection the value of the mass-average temperature ratio T_{ma} is 0.892 and the value of Fo is -0.0388 at the point of intersection. Assuming that a plot of the mass-average temperatures for the infinite cylinder passes through the same point with a slope appropriate for the infinite cylinder, the values of the mass-average temperature are in error by amounts of up to 4%. It may be noted from the graph of temperature distributions, p. 266, from Jakob (15) that distributions for the infinite cylinder depart most from the pattern of symetrical change for the distributions for geometries ranging from the sphere to the infinite slab. The 4% error would be the largest encountered for finite geometries considered in this report if we assume that all

mass-average temperature distributions converge. Such an assumption can be shown to yield valid information for a progression of ellipsoidal geometries smoothly changing from a sphere and approaching the infinite slab. Values of C for Equation 7 are easily determined for use in calculating values of T_{ma} for specified values of the exponent M_1^2Fo by the use of the cited coordinate values of the point of convergence.

Summary

The usual dimensional analysis for transient conduction heat transfer is extended by means of two orthogonal distance ratios to develop prediction equations that involve object geometry. The dimensionless analysis yields the prediction equation in general form,

$$T = f_1(Fo,Bi,L_d,A,B) \qquad (1)$$

where A and B are semi-major axes of an ellipsoidal model in units of the semi-minor axis.

The form of the prediction equation is shown to be,

$$T \equiv Ce^{-M_1^2Fo} \qquad (7)$$

where

$$C = f_2(A,B,Bi,L_d) \qquad (6)$$

$$M_1^2 = f_3(A,B,Bi) \qquad (10)$$

and

$$G = f_4(A,B) \tag{9}$$

The semi-log plot of temperature ratio versus the time index Fo has an apparent intercept denoted by the constant C. It appears that much of the disfavor of critics of the use of a single term approximation may be traced to uncertainty about the value of C. Values of M_1^2 determine the slope of the time-temperature relationship and is independent of L_d (Equation 10). A nomograph based on first roots of the transcendental equations for the infinite slab, infinite cylinder, and the sphere may be used to relate M_1^2 to G and Bi.

For anomalous shapes values of the geometry index G are predicted from values of A and B for the ellipsoidal model that replaces them by means of the equation

$$G = \frac{1}{4} + \frac{3}{8A^2} + \frac{3}{8B^2} \tag{14}$$

For brick shaped objects G is predicted by the equation

$$G = \frac{1}{4} + \frac{1}{4(s_2/s_1)^2} + \frac{1}{4(s_3/s_1)^2} \tag{12}$$

where s_1, s_2, and s_3 are semi-thicknesses of the brick (s_1 is shortest dimension).

For finite cylinders (length c and diameter d) G is predicted by the equation

$$G = 0.586 + \frac{1}{4(c/d)^2} \qquad (15)$$

CHAPTER IV

EXPERIMENTAL PROCEDURE

Introduction

An experiment was conducted with ellipsoidal shapes machined from acrylic plastic to compare the values of the geometry index G for the various shapes predicted by Equation 14 with those derived from time-temperature data from the shapes. Equation 7 was employed as the basis of evaluating thermal properties and values of G from time-temperature data. Shapes with the defined geometries of the sphere, cube, and cylinder (length = diameter) were used first to evaluate thermal diffusivity α for the plastic. Experimental conditions of negligible surface thermal resistance were used, i.e., $M_1^2 = G\pi^2$. Considering successive values of T and Fo gave the following relationship.

$$\alpha = \frac{\ell^2}{M_1^2} \left[\frac{\ln T_1 - \ln T_2}{\tau_1 - \tau_2} \right] \tag{16}$$

The slope of time-temperature data in each case was obtained by means of a regression analysis of data taken during the period of linearity of the transformed data. When a value of α was established for the plastic a similar form of the

equation was used with data from other plastic shapes,

$$G = \frac{\ell^2}{\alpha\pi^2}\left[\frac{\ln T_1 - \ln T_2}{\tau_1 - \tau_2}\right] \tag{17}$$

After establishing the validity of the method of geometry analysis, time-temperature data from anomalous shapes that were air-cooled was used to evaluate M_1^2 by the equation

$$M_1^2 = \frac{\ell^2}{\alpha}\left[\frac{\ln T_1 - \ln T_2}{\tau_1 \quad \tau_2}\right] \tag{18}$$

Through Equation 10 and the nomograph of Figure 3 values of surface conductance h were calculated from values of m.

Equipment Used

Equipment was designed and constructed to provide an agitated ice-water bath for cooling all the test shapes (Figure 4). Water was circulated over a bank of crushed ice at a flow rate sufficient to assure that the surface thermal resistance was negligible, i.e. the validity of Equation 8. The flow rate was adjustable to 70 gpm giving a mass flow rate through the container of about 30 gpm per square foot of cross-section. Calculations for spheres and cylinders with 2-inch radii indicated that values of surface conductance for these shapes would be at least 100 Btu/hr ft^2 °F based on a conservative estimate of the average free stream velocity of 6 ft/min. This value is sufficient to

assure a condition of negligible surface thermal resistance. When the equipment was operated at a flow rate of about one-half capacity, time-temperature data was obtained from plastic shapes that was not significantly different from that obtained with the higher flow rate. Fine frost was added intermittently to the container of ice water to insure a constant bath temperature of 32°F. The experiments were conducted in a room whose temperature was about 40°F to reduce heat gain to the bath equipment.

The Plastic Models

The plastic shapes were constructed with a basic minimum thickness of 3 inches or characteristic length of 1-1/2 inches. A small hole was drilled along the path of the characteristic length with a 7/64 inch drill to just admit 3 copper-constantan 36-gage thermocouples to the center and at 1/2 and 1 inch from the center. The thermocouples were set in this position in paraffin and sealed at the surface with plastic cement. The thermocouples permitted a monitoring of internal temperatures while heating the object in a constant-temperature water bath of approximately 110°F thermostatically controlled within a temperature range of about 1-1/2°F. A record of the temperature distribution was obtained during the cooling period. The object was suddenly moved from the constant-temperature environment to the cooling bath on the printing

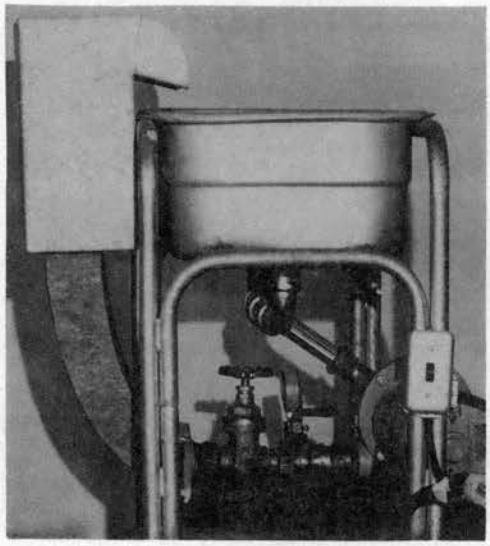

Side View

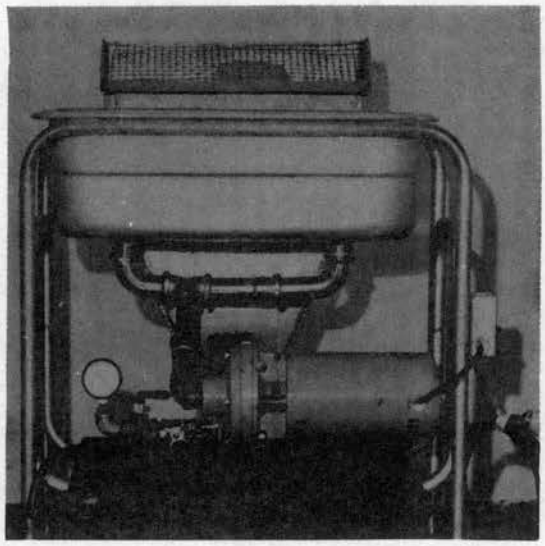

Front View

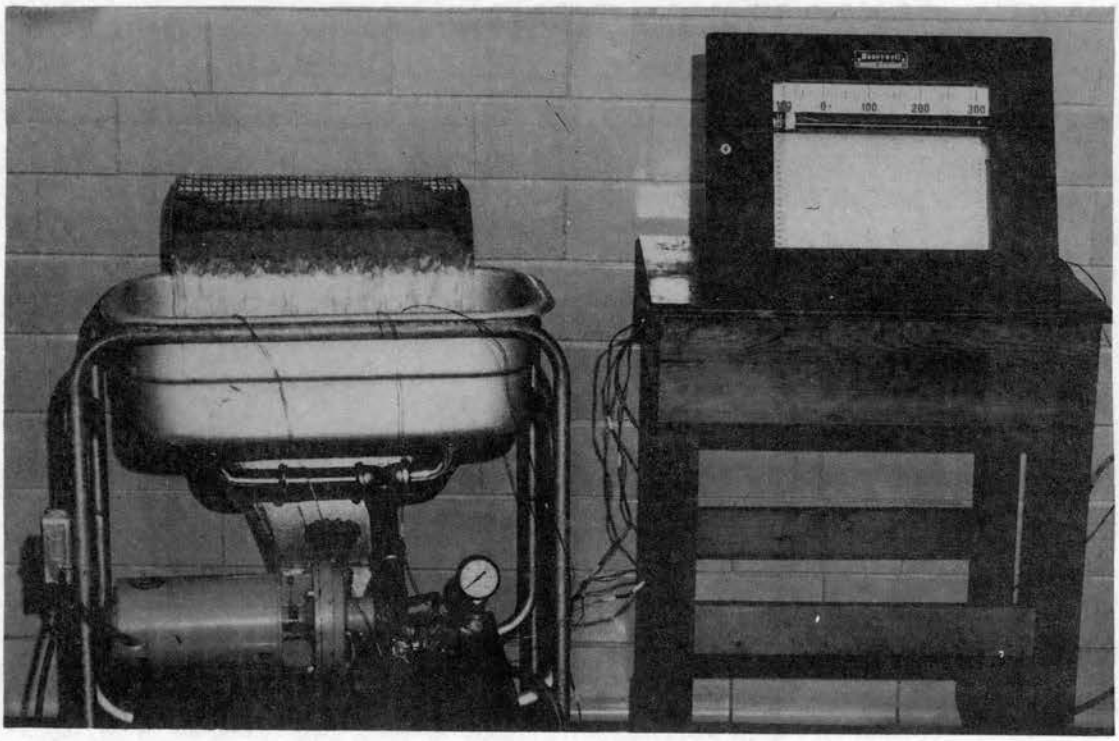

Figure 4. Views of equipment used to maintain a constant-temperature agitated cooling bath

of the temperature for the thermocouple at 1 inch from center. This minimized the overall effect of error in time for the points since the gradient is greatest during the time period of interest in the vicinity of the point 1 inch from center. Time-temperature slopes were derived from the data from this thermocouple. The slope of the time-temperature plot is independent of position on the characteristic length. However, transient temperatures near the surface are not considered suitable for prediction relationships. Because of the large time lag for the center and the unstable conditions near the surface, an intermediate point is most desirable. A 10-point recording potentiometer with a printing speed of 15 seconds between successive points was used to measure the temperatures. The temperature range of the recorder is -100°F to 300°F, calibration 2°F, and a specified accuracy of ± 0.8°F.

The plastic ellipsoidal shapes used were the prolate and oblate spheroids so that the shapes could be easily turned on a lathe. They were formed from patterns of accurately drawn ellipses. The semi-minor axes of the completed, polished shapes were measured to the nearest 1/64 inch. This dimension, the equation for volume of an ellipsoid, the weight, and formerly measured density of the plastic were used to calculate an average value of the semi-major axis for each shape. A single stock piece of

Grade "G" cast acrylic plastic was used for all the plastic shapes, excepting the first model made from the same type of material procured earlier. Values of the semi-major axes were chosen to provide a sampling of values of G over the full range of possible values. The set of 8 ellipsoidal shapes used in the study are shown in Figure 5.

Analog to Determine Characteristic Length

A plastic "loin strip" was constructed to serve as a more extreme example of an anomalous shape to test the methods of geometry analysis. This shape is illustrated in Figure 2. An experimental device was constructed to determine the characteristic length, the minimum distance spanned by the maximum temperature difference during the transient period of heat exchange.

The cross-sectional area designated as Area 1 in Figure 2 was selected to divide the mass of the object. If this area could be considered to be formed by a basic symetrical area with anomalous appendages of area distributed in a symetrical manner, the center of the basic area could be used to determine the characteristic length. This was not true for the plastic "loin strip" and, thus, the following device was constructed to experimentally locate the "source" of the isothermals for the transient period.

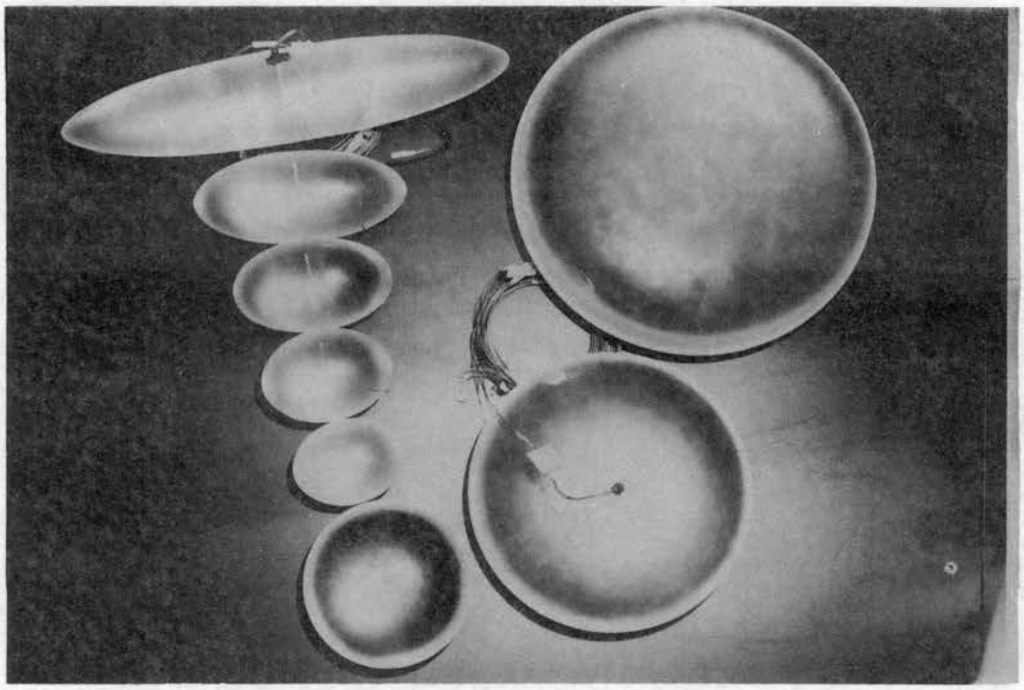

Top View

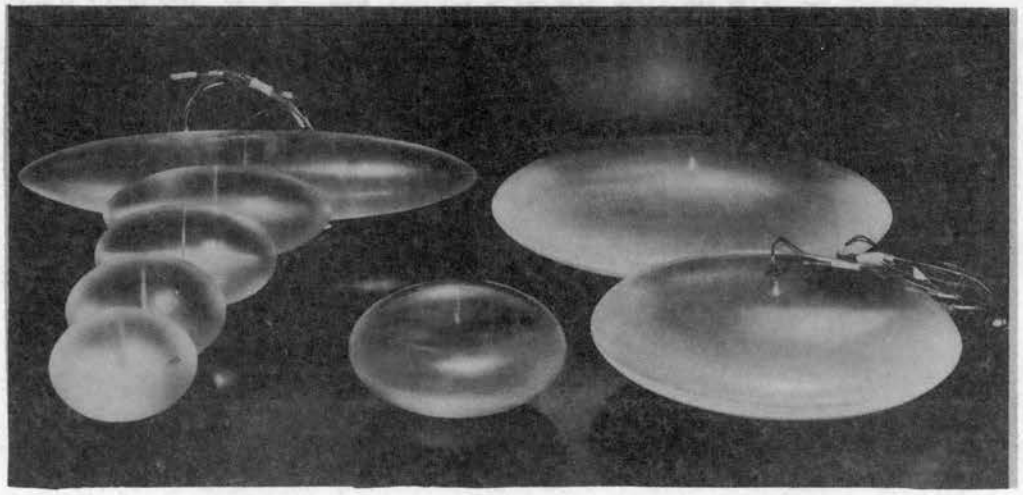

Front View

Figure 5. Acrylic plastic ellipsoids used for experimental measure of values of geometry index G

A line heat source was formed by encapsulating resistance wire into an asbestos surface so that the heat source had the shape of Area 1. An area with this shape was made of sheet copper so that the line heat source was in contact with the periphery of the copper area. A temperature sensitive paint with a temperature rating 100°F was used to coat the copper shape. Experiments were conducted to follow this isothermal of 100°F as it shrunk to locate the desired point. Characteristic length was determined as the single distance to the two points on the surface equidistant from the "source".

Temperature data from the plastic "loin strip" were obtained in essentially the same manner as that from the other plastic shapes. The slope of the time-temperature data yielded a value of geometry index G that was compared with the value predicted by Equation 14.

CHAPTER V

RESULTS OF THE EXPERIMENTS

Thermal Diffusivity for Acrylic Plastic

Values of thermal diffusivity, calculated from the experimental results by Equation 16, for the acrylic plastic are shown in Table II. The density of plastic was measured to be 74.3 lbs/ft^3 from the weights and volumes of the sphere, cylinder, and cube. This is the same value as is reported widely in commercial literature. Specific heat is widely reported to be 0.35 Btu/lb°F. Based on the measured value of α, a calculated value of conductivity is 0.117 Btu/hr°F ft. This compares with the single value sometimes reported in commercial literature of 0.12 Btu/hr°F ft. More often the conductivity for acrylic plastic is reported as 0.12 ± 20% Btu/hr°F ft, e.g. reference for values of thermal and physical properties (19). The magnitude of the variation introduced by experimental error in these measurements also may be observed in other tests with plastic material. The larger coefficient of variation (standard deviation/mean value) for the data from the sphere results from greater experimental error for the dimensions of the sphere. The cylinder and cube were constructed on a lathe

with more accuracy of the dimensions than the sphere. As expected, a significant increase in the coefficient of variation occurred for the data from heterogeneous materials.

TABLE II

THERMAL DIFFUSIVITY FOR ACRYLIC PLASTIC

Shape	Geometry Index G	Thermal Diffusivity Btu/hr°F ft.	Coefficient of Variation	Number of Runs
Sphere	1.000	4.49×10^{-3}	1.60%	4
Cylinder	0.836	4.50×10^{-3}	1.31%	8
Cube	0.750	4.51×10^{-3}	1.37%	8
All Values	---	4.50×10^{-3}	1.35%	20

Geometry Data from Plastic Ellipsoids

Data for the eight plastic ellipsoids are summarized in Table III. It is clear from the experimental results that the prediction equations for values of G are valid over the complete range of ellipsoidal shapes. Since values of G range from 1.00 to 0.25, the experimental data covers the full range of possible values. Percentage differences between predicted and experimental values of G are under 1% for all cases.

The mean time-temperature data from 7 determinations for the plastic ellipsoids is summarized in Table IV. This same information is graphically displayed in Figure 6. In order for a clearer comparison to be possible from this data the regression line was shifted so that the mass-average temperature ratio T_{ma} of each shape is indicated.

TABLE III

GEOMETRY DATA FROM ACRYLIC PLASTIC ELLIPSOIDS

No.	Characteristic Length ℓ, Feet	Distance Ratio A	Distance Ratio B	Predicted Geometry Index G Eqn. 14	Experimental Geometry Index G	Coefficient of Variation*
1	0.115	1.00	1.28	0.854	0.858	0.86%
2	0.126	1.00	1.34	0.834	0.837	1.46%
3	0.126	1.00	1.70	0.755	0.754	0.88%
4	0.125	1.00	2.30	0.696	0.691	0.61%
5	0.129	1.00	5.01	0.640	0.639	0.61%
6	0.126	1.76	1.76	0.492	0.491	0.81%
7	0.126	2.97	2.97	0.335	0.335	1.70%
8	0.126	4.00	4.00	0.297	0.295	1.25%

*Coefficient of variation obtained from 7 determinations.

TABLE IV

TIME-TEMPERATURE DATA FROM ACRYLIC PLASTIC ELLIPSOIDS

Time, τ Hours	Temperature Ratios* T for Ellipsoids 1	2	3	4	5	6	7	8
0.333	0.197	-----	-----	-----	-----	-----	-----	-----
0.417	0.154	0.280	0.360	0.346	0.366	0.398	0.389	0.408
0.500	0.121	0.231	0.300	0.293	0.315	0.352	0.356	0.379
0.583	0.097	0.190	0.252	0.247	0.272	0.313	0.378	0.353
0.667	0.075	0.156	0.214	0.211	0.234	0.282	0.303	0.328
0.750	0.060	0.127	0.179	0.180	0.203	0.251	0.280	0.307
0.833	0.047	0.106	0.147	0.153	0.177	0.225	0.260	0.288
0.917	0.037	0.086	0.124	0.129	0.152	0.199	0.241	0.267
1.000	0.029	0.072	0.105	0.109	0.130	0.178	0.224	0.252
1.083	-----	0.059	0.088	0.093	0.113	0.158	0.208	0.234

*Each temperature ratio is average of 7 determinations.

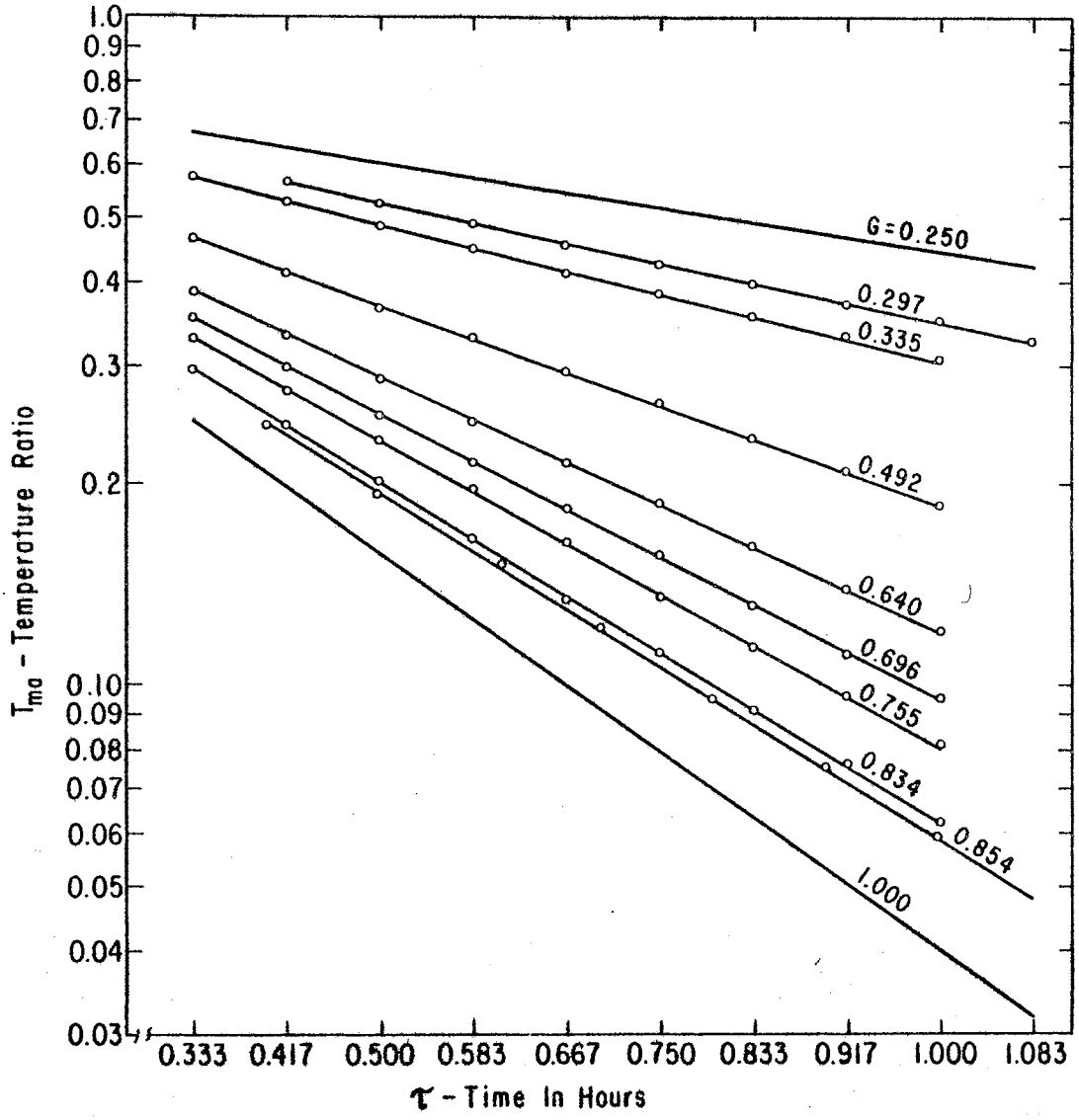

Figure 6. Mass-average temperature ratios versus time for acrylic plastic ellipsoids

The slope from the regression analysis and the mean value of Fo were used to calculate a mean log temperature ratio for the data points. A mass-average temperature ratio for this slope and value of Fo were calculated as indicated on Page 30. The difference between the values of log temperature ratio were added or subtracted, as appropriate, to the values of log temperature ratio for all the data points. Variation of the data points about the shifted regression line was not altered. Plots of time-temperature slopes for the infinite slab and the sphere are given for comparison (taken from graphs on Pages 101 and 234, Carslaw and Jaeger [5]). The data for ellipsoid Number 1 (Table III) with G = 0.854 was further adjusted to indicate data for an ellipsoid with this geometry index and a characteristic length of 1-1/2 inches. This particular shape was the first one of the set made and was formed from a 1-3/8 inch radius plastic cylinder before the stock material was received.

The results of the treatment of the data shown in Figure 6 give strong support to justify the approximation procedure for predicting mass-average temperature ratios as a function of geometry (p. 30). It may be noted that the value of L where T_{ma} occurs has not yet been considered. The location of the temperature ratio is different for the different ellipsoids as determined by the direction of the shifting required to obtain the given plots.

Mass-Average Temperature and Geometry Index

The temperature data for the ellipsoids for a time of 0.708 hours was selected (so that the value of Fo is 0.2) and used to compare temperature distributions for all the plastic shapes. The temperature ratios of the three interior points and the surface temperature were used to construct the distributions shown in Figure 7. Distributions for the sphere and infinite slab are shown for comparison. Information about the location of the mass-average temperatures for the sphere, infinite cylinder, and infinite slab was obtained from the graph, p. 102, in Carslaw and Jaeger (5). The mass-average temperature ratios for the ellipsoids was predicted from the assumption of convergence of the semi-log plots of time-temperature data for all the shapes as described on Page 30. Placing the predicted mass-average temperature on the distribution for each shape indicates the location along the characteristic length L_{ma} where the temperature ratio occurs. Similar plots of distributions at other values of Fo serve to indicate that this location remains stable for a given shape as indicated earlier for the spherically shaped objects (25) and from theoretical calculations (5).

The inset of Figure 7 shows the relationship between geometry index G and the location L_{ma} of the mass-average temperature. The equation,

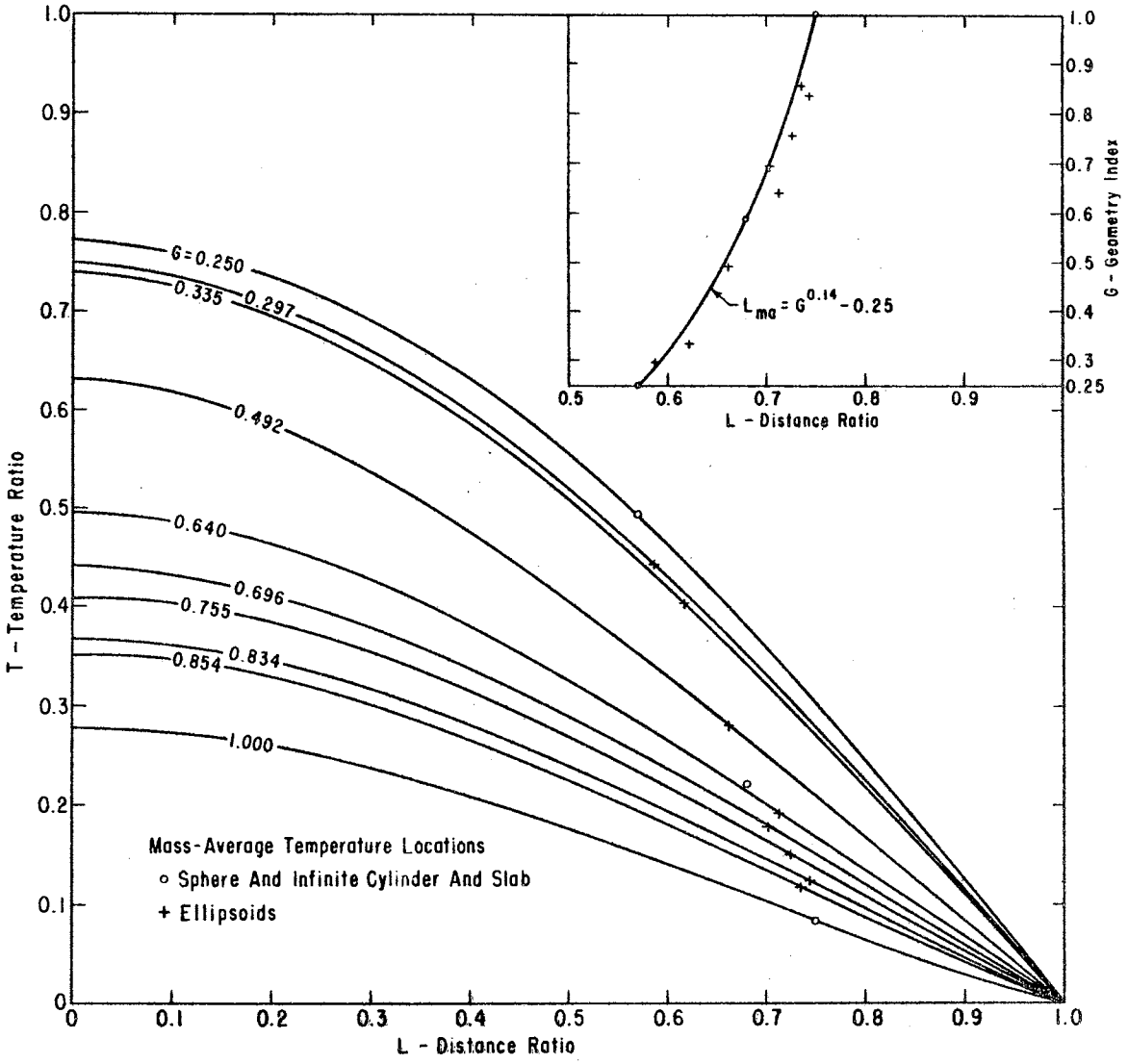

Figure 7. Temperature distributions for plastic ellipsoids at Fo = 0.2. Object mass-average temperature ratios are located on distributions. Inset shows T_{ma} location versus G

$$L_{ma} = G^{0.14} - 0.25 \qquad (19)$$

was derived to fit the data points for the sphere, infinite cylinder and infinite slab. The experimental data from the ellipsoids serve to confirm the validity of the equation. The accuracy of locating the thermocouple along the characteristic length as compared to the accuracy of measure of ℓ to the nearest 1/64 inch is but one source of error that causes uncertainty in this data. The data is presented as supporting evidence to that of reference (5) to show that the location of the mass-average temperature can be related to object geometry.

Data From Anomalous Shapes

Data From "Plastic" Ham

In order to compare predicted and experimental values of the geometry index G for anomalous shapes a plastic model of a boneless ham was constructed with shape and dimensions of a typical ham. Geometry data for the ham were: ℓ = 0.123 ft., A = 2.74, B = 4.30, and G = 0.320. Cooling tests were conducted with this shape in essentially the same way as with the earlier plastic shapes. The logarithm of temperature ratio versus time for the shape decreased linearly for a time. Then, other effects began to influence the cooling rate to produce a slower cooling rate. Since it was more difficult to bathe the entire surface in the agitated bath it was first suspected that an increase in surface thermal

resistance produced this effect. Higher flow rates through the pan were used, the shape was positioned to more favorably apply the stream velocity across the surfaces, and, finally, the shape was manually agitated in the agitated bath. None of these efforts were effective in changing the pattern of the time-temperature distribution. It is hypothesized that volumetric expansion of the "plastic" ham caused a shift in the location of the thermocouple with respect to characteristic length to produce this result. The time-temperature distribution for this object is shown in Figure 8. The slope of the distribution during the initial linear trend of the data yields a value of G of 0.317 as a mean value of 7 runs. The difference in the predicted and experimental values of G are well within the range of such values for the ellipsoidal shapes. It is interesting to note that if we consider the geometry of the parallelopiped from which the shape was constructed, Equation 12 predicts a value of G of 0.317 and Equation 14 for the ellipsoidal equivalent predicts G = 0.311.

Data From "Plastic" Loin Strip

The substance of the results from the analog experiment to determine the characteristic length for the "plastic" loin strip is shown in Figure 9. The anomalous area in this experiment was approximately four times the area from the plastic shape. Thus, the location of the "source"

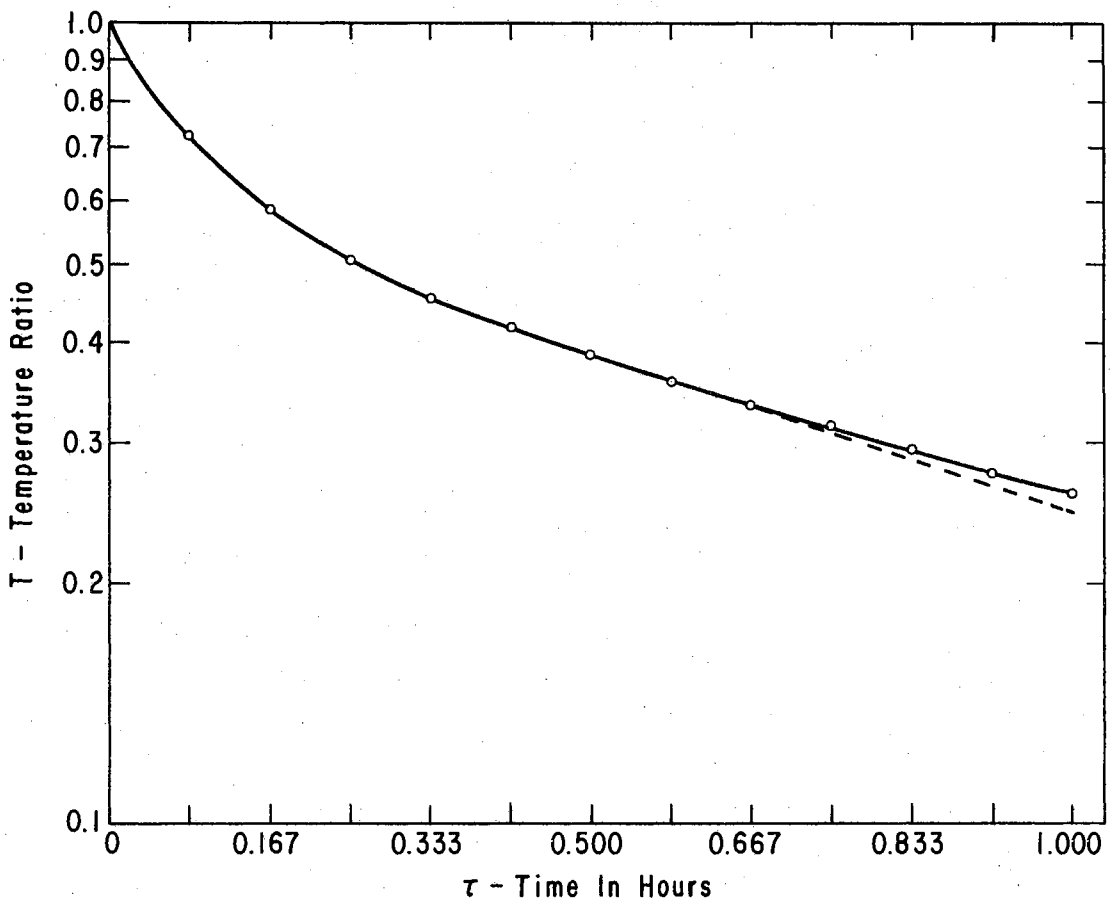

Figure 8. Temperature ratio versus time for a "plastic" ham. The dashed line denotes the initial linear trend of the data

of isothermals is expressed as a ratio of the radius r for the circle O that forms the basis of the anomalous area. The point P is located at a distance 0.246r away from O for all areas that are geometrically similar to the tested area.

The "plastic" loin strip was made in the form of a truncated cone with a length of 12 inches. The three geometrically similar areas involved are described in Table V. They are the end planes and the longitudinal plane that divides the mass. This plane is 6.5 inches from the small end.

TABLE V

DATA FOR PLANES OF "PLASTIC" LOIN STRIP

Plane	Radius, r Inches	Area Sq. Inches	Length, ℓ Inches
Small End	1.50	11.53	1.33
Central	----	14.04	1.48
Large End	1.80	16.16	1.60

The end planes were chosen with radii as indicated and used to construct the characteristic shape based on the circle O. The location of P on the end planes was positioned according to Figure 9 at a distance of 0.246r from point O. Values of the length ℓ were measured for the end planes. Values of the end-plane areas were measured with a polar planimeter and other values of area were assumed to be a linear function of the cone length. The equation

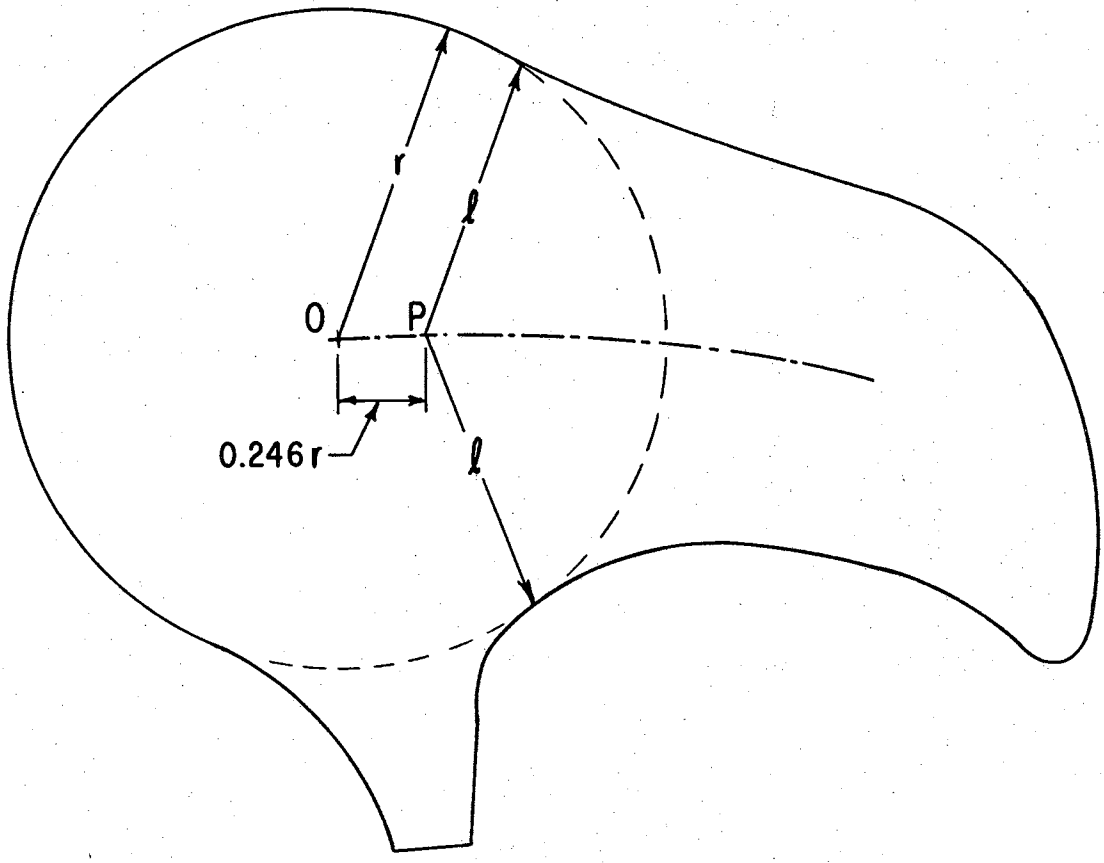

Figure 9. Area 1 for the "plastic" loin strip with results of the experiment to evaluate characteristic length ℓ

for the volume of a truncated cone was used in a "cut and try" solution to determine the plane that divides the volume. Values of the cross-sectional area were assumed to be of the form

$$\text{Area} = \phi \ell^{\kappa} \tag{20}$$

Values of the end-plane areas were used to evaluate the constants: $\phi = 6.84$ and $\kappa = 1.83$ Then, the characteristic length ℓ for the object was determined by Equation 20 and the value of the area of the plane dividing the mass.

A mean value of the time-temperature slope, using regression analysis, for 7 determinations for the loin strip was 1.0583 hr^{-1} ± 1.29%. Using this value with the determination of ℓ and the diffusivity of acrylic plastic of 0.0045 ft^2/hr determined earlier substituted in Equation 17 gives a value of G of 0.362. Completing the geometry analysis for the shape from data in Table V, the values of A and B are 2.04 and 5.11, respectively. By Equation 14, the predicted value of G is 0.355. This represents a percentage difference of 2.0% between predicted and experimental values of G. This difference is just slightly larger than that obtained for the plastic ellipsoids. The "plastic" loin strip, then, provides excellent validation of the proposed use of the ellipsoidal model to replace the anomalous shape in describing transient conduction heat transfer from the anomalous shape.

To further examine the results of the analog experiment, thermocouples were placed at points O and P in the central plane dividing the mass of the shape. During transient cooling of the object the temperature at point O was slightly larger than that at point P for the early period of time when the plot of time versus lnT is nonlinear. For greater values of time the temperature at point P was less than that at point O.

Thermal Diffusivity of Hams

A total of 21 measurements were made of the thermal diffusivity α for that number of specimens of the boneless processed hams. These hams are fully cooked and are vacuum packed in a fibrous cellulose container of 3 mils thickness and a plastic container of 1/2 mil thickness. The thermocouple probe used with the hams was made up with three thermocouples spaced 1/2 inch apart and encased around the periphery of a 1/8 inch diameter plastic rod within 3 coats of a plastic dipping compound. The thermocouple probe was inserted into the ham along the characteristic length with a thermocouple at the center of the ham. Geometry analysis was made from three overall dimensions from the ham. Minimum semi-thickness gave the characteristic length ℓ. The smaller cross-sectional area was assumed to be composed of two semi-circles (2ℓ = diameter) joined by a rectangle.

The larger cross-section was assumed to be rectangular. Calculation of values of G were made according to the plan illustrated in Figure 1.

The data for measuring thermal diffusivity for the processed hams is given in Table VI. On the basis of the variations to be expected among specimens we might expect some variation in values of the thermal properties. And, on the basis of possible sources of experimental error a large coefficient of variation could be expected. Sources of experimental error include: possible location of thermocouple in void or gelatin pocket, large volumetric expansion over temperature range (110°F to 32°F), shifts in geometry because of pliable nature of product, the difficulty in making accurate length measurements (especially characteristic length), and the experimental error in measuring temperature values. The difficulty encountered with the time-temperature data from the "plastic" ham was not noticed in the data from the processed hams. The data period was for a longer period of time (reflecting the different magnitude of ℓ in the value of Fo) and no tendency was noted for the slope to change after the initial linear portion of the time-temperature relationship was established.

No reported values of diffusivity for cooked ham have been found in the literature to form a basis of comparison. On the basis of reported values of conductivity for raw lean pork some confirmation of the work is obtained. Lentz

TABLE VI

DATA FOR THERMAL PROPERTIES OF BONELESS PROCESSED HAMS

Geometry Index G	Time-Temp Slope, Hr^{-1}	Length, ℓ Ft	Density, ρ Lbs/ft^3	Diffusivity, α Ft^2/hr	Conductivity*, k Btu/hr°F ft
0.371	0.634	0.150	66.9	3.89×10^{-3}	0.233
0.379	0.546	0.163	67.0	3.88	0.232
0.385	0.555	0.158	67.2	3.65	0.219
0.387	0.567	0.158	66.8	3.70	0.221
0.389	0.521	0.163	67.0	3.60	0.216
0.391	0.548	0.158	66.8	3.54	0.211
0.392	0.530	0.163	67.0	3.64	0.218
0.400	0.493	0.171	65.3	3.64	0.212
0.400	0.545	0.163	65.8	3.66	0.215
0.413	0.523	0.169	66.8	3.66	0.219
0.418	0.537	0.169	66.8	3.71	0.222
0.419	0.527	0.175	67.3	3.89	0.234
0.423	0.520	0.171	65.8	3.63	0.214
0.427	0.518	0.175	66.8	3.76	0.225
0.427	0.517	0.177	66.0	3.84	0.227
0.430	0.451	0.177	66.3	3.33	0.197
0.439	0.504	0.179	67.2	3.72	0.223
0.445	0.481	0.181	66.8	3.59	0.214
0.454	0.505	0.181	66.5	3.70	0.220
0.454	0.451	0.181	66.9	3.30	0.197
0.464	0.514	0.183	67.5	3.75	0.226
Average of 21 values				3.67×10^{-3}	0.219
Coefficient of variation				4.2%	4.5%

*Conductivity is based on specific heat of 0.894 Btu/lb°F.

(17) reports a value of about 0.28 Btu/hr°F ft for unfrozen raw lean pork at 32°F. Olson and Schultz (22) report a value of 5.00×10^{-3} ft^2/hr for α for a canned spiced ham processed in 1942 from which a value of k is calculated to be 0.24 Btu/hr°F ft. This gives a clue that values of k are smaller for cooked pork (with processing liquids added) than the raw lean pork.

A calorimeter was used to measure the specific heat of samples of the processed hams. For 16 determinations a mean value of 0.894 Btu/lb°F was obtained with a coefficient of variation of 3.2%. The mean value of specific heat was used with density, obtained from water displacement data, and diffusivity for each of the 21 hams to calculate values of conductivity. These results are included in Table VI. The processed hams used in this study had a fat content of about 10% based on routine laboratory determinations of fat content of hams processed in the same way over a period of several years. Processing of the hams include deboning, defatting, injection with a curing brine, and heating to an internal temperature of 155 to 160°F.

Volume Relationships for Ellipsoids

A relationship between an ellipsoid and the equivalent parallelopiped (i.e., orthogonal cross-sectional areas are equal) was employed as a useful check on the measurement of

the dimensions of the ham. For the volume of the ellipsoid we have

$$V_e = \frac{4\pi \ell^3 AB}{3} \tag{21}$$

The cross-sectional area of the smaller ellipse is $\pi \ell^2 A$. The equivalent rectangular area is $4\ell s_2$ (s is semi-thickness and $s_1 = \ell$). Thus, $s_2/\ell = A\pi/4$. Similarly, $s_3/\ell = B\pi/4$. For the volume of the parallelopiped we have

$$\begin{aligned} V_p &= 4(2\ell \times s_2 \times s_3) \\ &= 8\ell^3 \left[\frac{s_2}{\ell} \times \frac{s_3}{\ell}\right] \\ &= \frac{\ell^3 \pi^2 AB}{2} \end{aligned} \tag{22}$$

The ratio V_p/V_e is 1.178. The relation used is that the volume of the equivalent parallelopiped is 17.8% greater than the ellipsoid. It was found that the weight of hams were from 8% to 12% more than the calculated weight of the ellipsoidal model representing the shape of the ham. On some occasions apparently anomalous diffusivity measures were brought within the overall range of the data by a remeasure of object diamensions when this volume ratio was observed to fall outside this range of 8% to 12%. The volumes of anomalous shapes that lend themselves to geometry analysis would necessarily fall in the range of 100% to 117.8% of the ellipsoidal models that replace them.

Surface Conductances for Hams

Time-temperature data from 38 of the processed hams subjected to air cooling was obtained during August, 1965. The process operation of heating raised the center temperature of the hams to about 160°F. The assumption of uniform initial temperature was not obtained; however, the slow heating rate produced final distributions with small gradients. The distributions were examined to subjectively estimate the initial object mass-average temperature. They were cooled three at a time in a small laboratory rapid-cooling cabinet with a chamber size of 2' × 2' × 2'. Air movement in this space is turbulent and an effective approach velocity of the air is difficult to evaluate. Based on measurements, with a rotating-vane anemometer, of air velocities in the space a value of 120 fpm was determined as the effective approach velocity. Temperatures were obtained by means of the thermocouple probes that indicated the temperature at the center and at 1/2 and 1 inch from center along the characteristic length. The time-temperature slope was obtained from the thermocouple 1 inch from center, the recorded temperature nearest the mass-average temperature of the ham. Geometry analysis was based on three dimensions taken from each ham as described earlier.

Using the time-temperature slope from regression analysis of the time-temperature data, the value of

thermal diffusivity measured for the hams, and the characteristic length, a value of M_1^2 was evaluated according to Equation 18. The value of M_1^2 and geometry index G were used with the nomograph, Figure 3, to determine m and from $m = k/h\ell$ a value of h was calculated. The results are given in Table VII.

TABLE VII

EXPERIMENTAL VALUES OF h FOR PROCESSED HAMS WITH AIR VELOCITY OF 120 fpm AND INDICATED TEMPERATURE

Air Temperature °F	Number of Determinations	Mean h Btu/hr°F ft^2	Coefficient of Variation
-10	18	3.59	11.4%
-55	3	3.60	5.8%
-60	3	3.47	12.4%
-70	9	3.52	8.5%
-80	5	3.20	8.8%

The data period times for measuring surface conductances extended to 2-1/4 hours for the warmer temperatures and to 1-1/2 hours for the colder temperatures. The cooling time was adjusted so that the final mass-average temperature of the ham was about 45°F. It was observed that freezing of the hams was just commencing for air temperatures of -10°F and 2-1/4 hours of cooling and for -80°F cooling temperature freezing of the surface began to occur at about 1 hour.

There was no significant difference because of temperature change between the measured values of surface conductance except the values at the lowest temperature.

Test conditions were held essentially constant except for the variation in temperature of the cooling air. The following calculations are given to indicate the influence of the change in the properties of the cooling air upon the value of surface conductance. From Eckert and Drake (7), p. 242, we have an equation relating the Nusselt number, $Nu = hd/k_a$, and the Reynolds number, $Re = du/\nu$, for a horizontal cylinder with convection heat exchange in air when Re is in the range 40-4000. The cylinder diameter is d, conductivity of air is k_a, u is the air velocity, and ν is kinematic viscosity. From the equation we can get the proportionality,

$$h \propto \frac{k_a}{\nu^{0.466}} \tag{23}$$

if we assume that all other quantities are constant as we consider different air temperatures. Consider the influence of these properties of air for two reference temperatures of 70°F and 0°F that cover the range of conditions used with the hams. The properties of the air at 70°F are $k_a = 0.0148$ Btu/hr°F ft and $\nu = 1.63 \times 10^{-4}$ ft^2/sec and for 0°F air $k_a = 0.0133$ Btu/hr°F ft and $\nu = 1.30 \times 10^{-4}$ ft^2/sec from the same reference. Let the subscripts 1 and 2 denote the temperatures 70°F and 0°F. Then we may determine if we have the equality

$$\left(\frac{k_a}{\nu^{0.466}}\right)_1 = \left(\frac{k_a}{\nu^{0.466}}\right)_2$$

or

$$\frac{k_{a,1}}{k_{a,2}} = \left(\frac{\nu_1}{\nu_2}\right)^{0.466} \tag{24}$$

When we substitute values we have the following,

$$\frac{0.0148}{0.0133} = \left(\frac{1.63\times10^{-4}}{1.30\times10^{-4}}\right)^{0.466}$$

$$1.11 = (1.25)^{0.466}$$

$$1.11 = 1.11$$

This result serves to explain the constant values of h experimentally determined for the hams.

The lower values of h for the -80°F air temperature is not a result of the change in temperature but a consequence of the surface freezing occurring for this object. Thermocouples placed on the surfaces of the hams during cooling gave temperatures that indicate that there is a moderating influence from the freezing upon the decrease in surface temperature by the sub-freezing air. The release of latent heat at the surface during the phase change causes this. From the standpoint of conduction heat transfer, then, the full temperature potential is not available to remove sensible heat from the interior of the object. This brings about the lower value of h or apparent increase in thermal resistance at the surface. This is only part of the overall heat exchange process. The actual amount of heat removed is greater for the object because of surface

freezing. The method of evaluation based on transient conduction heat transfer is insensitive to the amount of heat involved in the fusion process. Other methods will have to be devised to evaluate the total heat exchange process.

CHAPTER VI

DISCUSSION AND CONCLUSIONS

Discussion

The use of available time-temperature charts for solving practical problems in transient conduction heat transfer has been greatly hampered by the lack of information about the thermal properties of many materials of interest. Typically a user "guesstimates" the thermal properties of a material and makes coarse assumptions regarding the geometry of the shape. These handicaps coupled with the frequent "cut and try" methods of problem solving do not inspire confidence in or encourage use of the time-temperature charts. Actually, when accurate information is used with the charts accurate answers can be obtained. Anyone who has taken data under conditions that satisfy the assumptions on which the charts are based knows the dependability of the results predicted by the charts. The method of geometry analysis presented in this report is given to implement the use of the available time-temperature charts.

In the first place, the use of geometry analysis can bring about the accumulation of accurate information about

the properties of diffusivity, conductivity and surface conductance for many materials that occur in anomalous shapes and do not lend themselves to study by presently used methods. For example, we are interested in these properties for a loin strip. Even if we know conductivity, density, and specific heat for bone, fat, and muscle tissues and the proportions of each, uncertainty would exist about a computed value of diffusivity. In many cases, such as with the meat products, anisotropy of thermal conductivity is an added complication. Preliminary work with the loin strip indicates that this shape will yield to the method of geometry analysis for evaluating the thermal properties.

A quotation from a report of Heisler (12) in 1946 points to a condition that still exists. He says, "In many instances the engineer has little to use as a guide and the boundary resistance in his calculations may then largely be the result of concentrated wishful thinking." Geometry analysis used with the nomograph of this report and prior measurement of diffusivity and conductivity can be useful in measuring surface conductance for different shapes and external conditions. Reports of average values of h most often indicate uncertainties of ± 20% with definable geometries such as the sphere and cylinder. The coefficient of variation of about 11% for values of h for processed hams looks impressive in comparison.

Secondly, the use of geometry analysis will be useful in the solution of problems with the time-temperature charts where thermal properties are known but we have the geometry anomaly. The use of the nomograph of Figure 3 with definable shapes such as finite cylinders and bricks will replace the so-called "product solution" and the "cut and try" solutions. To illustrate this refer to the solution of Example 4-3, p. 88, Eckert and Drake (7). In summary the problem is: What value of time τ is required for a value of T of 0.0735 for the center of a steel brick 2' × 2' × 4' when α = 0.570 ft^2/hr, k = 25 Btu/hr°F ft and h = 100 Btu/hr°F ft^2? From Equation 12, G = 0.563 and from the given data, $m = k/h\ell = 0.25$. On the nomograph align G = 0.563 with m = 0.25 and read $M_1^2 = 3.59$. Recalling that Equation 7 serves for all geometries refer this problem to the Heisler time-temperature chart for the sphere for which G = 1.00. Pivot on $M_1^2 = 3.59$ and align with G = 1.00 and read m = 0.63. From the Heisler chart for the central values of T for a sphere where T = 0.0735 and m = 0.63 read Fo = 0.87. From $Fo = \alpha\tau/\ell^2$ solve for τ = 1.53 hours, the answer sought and the answer obtained in Eckert and Drake by the "cut and try" and "product solution" methods.

Many of the practical problems encountered may be solved by means of the nomograph and the Heisler charts for the sphere. (For conditions of large m the chart for

the slab may be similarly used.) The approximately straight lines of the time-temperature chart are predicted by Equation 7. Values of C and M_1^2 determine the particular line that is described. Equation 18 illustrates that the experimental evaluation of M_1^2 is independent of C. Comparing the charts for the infinite slab and sphere, in at least one case where M_1^2 is the same for the two geometries, values of C are also identical. The line for m = 0 from the slab is identical to the line for m = 1 from the sphere. In all other cases when M_1^2 is the same for these different geometries, the differences in corresponding values of C are so small that values of temperature ratios are not different within the readability of the charts. This property appears to be valid for center temperatures for the different geometries. It is less valid for predicting temperatures at locations along the characteristic length where the temperature of interest occurs at identical fractional parts of ℓ for the sphere and the object of interest. The most dependable use of the relationship, however, is in predicting mass-average temperatures for different geometries where the location of the temperature on the characteristic length varies with geometry as described by Equation 19.

Finally, the information about the location of the mass-average temperature should prove to be valuable in practical applications. While the error in temperature is

greater by missing its location than it is for a miss of the same distance in locating the position of the center temperature, it is often of considerable interest to know where to attempt a temperature measurement that gives a guide to the relative quantity of heat contained in the object during transient exchange. For predictions about the mass-average temperature for a shape of given G value, the problem is referred to the chart for a sphere at a location of L_{ma} = 0.75L and the solution obtained gives the mass-average temperature of the given shape. The "Position Chart" of Heisler (13) facilitates this solution. A time-temperature chart in the manner of Heisler for the mass-average temperature of a sphere for the different values of Bi would be valuable for solutions of this kind of problem.

Conclusions

1. The ellipsoidal model is the most valid model and one that adapts itself with the greatest facility for use in replacing a large range of anomalous shapes for predictions in transient conduction heat transfer.

2. A geometry index G is very useful in representing the geometry of a wide range of geometrical shapes. Its definition is based on the first term of infinite series solutions and the conditions of negligible surface thermal resistance.

3. A nomograph is valid in extending the concept of the geometry index to conditions of finite internal and surface thermal resistance.

4. A prediction equation involving two distance ratios for the anomalous shape gives an accurate index of object geometry.

5. For the shapes of defined geometry of the finite cylinder and brick equations from the literature yield values of geometry index G.

6. Values of G for characteristic anomalous shapes in which many materials occur may be used with time-temperature data obtained under the conditions of negligible surface thermal resistance to measure thermal diffusivity.

7. A powerful method of evaluating average surface conductances for anomalous shapes is provided by the method of geometry analysis and the nomograph developed in this study.

8. The location of the mass-average temperature of an object during the period of transient heat transfer may be related to the value of geometry index G by means of an equation developed in this study.

9. The use of the concept of geometry index and the nomograph relating G, Bi, and a function of the time-temperature slope contributes to a unified and rational approach to problem solutions in the area of transient

conduction heat transfer based on existing graphical solutions in the form of time-temperature charts.

CHAPTER VII

SUMMARY

The need for information about the thermal properties of commercial cuts of pork stimulated research on the effect of geometry of anomalous shapes on the transient heat transfer from such objects. An approximation method for evaluating the geometry of these shapes would permit the measurement of thermal properties of many products of interest and with the properties known be used in a rational approach to problems of transient heat transfer from the anomalous shapes.

In order to evaluate the geometry of an anomalous shape it is necessary to do this in terms of a model that would adequately replace the object. The objectives of the study were to derive a model and a parameter G to denote geometry. In terms of measurements from the anomalous shape, the parameter G was to be predicted. Experiments were conducted to test the validity of using the geometry index G in predicting internal temperatures for the model and anomalous shapes. Thermal properties of anomalous shapes were measured.

An ellipsoidal model was used to replace the anomalous shapes. Dimensionless ratios A and B give the lengths of

the semi-major axes, in units of a characteristic length ℓ, for the ellipses that define the general ellipsoid. The minimum semi-thickness of the object and model is the characteristic length. Orthogonal areas in planes of ℓ are equal for the model and the anomalous shape. A geometry index G was defined in terms of the parameters A and B and predicted for the ellipsoidal model by the following equation:

$$G = \frac{1}{4} + \frac{3}{8A^2} + \frac{3}{8B^2}$$

Values of G for anomalous shapes serve as an index of geometry and may be used in evaluating thermal properties of products occurring in the anomalous shapes. Knowledge of G is also useful in predictions for different shapes in conjunction with graphical solutions in the form of time-temperature charts for transient heat transfer.

Data was obtained to validate the prediction equation for the ellipsoidal model and for anomalous shapes. Experimental temperature distributions were used to relate the location of the mass-average temperature to the geometry index G.

The boneless processed ham was used as an example of an anomalous shape for the use of time-temperature data and geometry analysis to measure thermal diffusivity. With diffusivity and conductivity known for the processed ham,

time-temperature data obtained during air cooling was used to evaluate surface conductance for specified conditions. Applications of the concept of geometry analysis for anomalous shapes, when thermal properties are known, was presented.

A SELECTED BIBLIOGRAPHY

(1) Ball, C. O. and F.C.W. Olson. Sterilization in Food Technology-Theory, Practice, and Calculations. McGraw-Hill Book Co., New York, 1957.

(2) Bennett, A. H. Thermal Characteristics of Peaches as Related to Hydrocooling. USDA-AMS Technical Bulletin No. 1292, 1963.

(3) Buckingham, E. On Physically Similar Systems. Phys. Rev. 4:345, 1914.

(4) Carslaw, H. S. Introduction to the Mathematical Theory of the Conduction of Heat in Solids. 2nd Edition. MacMillan and Co., London, 1921.

(5) Carslaw, H. S. and J. C. Jaeger. Conduction of Heat in Solids. Oxford University Press, London, 1959.

(6) Dickerson, Roger W., Jr. An Apparatus for the Measurement of Thermal Diffusivity of Foods. Food Technol. 20:880-886, 1965.

(7) Eckert, E.R.C. and R. M. Drake, Jr. Heat and Mass Transfer. McGraw-Hill Book Co., New York, 1959.

(8) Fourier, J.B.J. Théorie Analytique de la Chaleur, Paris, 1822. English translation by A. Freeman, Cambridge, 1878.

(9) Gane, R. Thermal Conductivity of the Tissue of Fruits. Ann. Rept. Food Investigators Board Great Brit. 211, 1936.

(10) Gurney, H. P. and J. Lurie. Charts for Estimating Temperature Distributions in Heating or Cooling Solid Shapes. Ind. Eng. Chem. 15(11): 1170-1172, 1923.

(11) Haji-Sheikh, A. Application of Monte Carlo Methods to Thermal Conduction Problems, Unpublished Ph.D. Thesis, University of Minnesota, 1965.

(12) Heisler, M. P. Temperature Uniformity in Heating-up Process. Trans. ASME 68:493-502, 1946.

(13) Heisler, M. P. Temperature Charts for Induction and Constant-Temperature Heating. Trans. ASME 69: 227-236, 1947.

(14) Ingersoll, L. R., O. J. Zobel, and A. C. Ingersoll. Heat Conduction With Engineering and Geological Applications. McGraw-Hill Book Co., New York, 1954.

(15) Jakob, Max. Heat Transfer Vol. I, John Wiley & Sons, Inc., New York, 1949.

(16) Kirkpatrick, E. T. and W. F. Stokey. Transient Heat Conduction in Elliptical Plates and Cylinders. Trans. ASME, J. of Heat Transfer 81(C-1):54-60, 1959.

(17) Lentz, C. P. Thermal Conductivity of Meats, Fats, Gelatin Gels, and Ice. Food Technol. 15: 243-247, 1961.

(18) Miller, Herbert L. and J. Edward Sunderland. Thermal Conductivity of Beef. Food Technol. 17:490-492, 1963.

(19) Modern Plastics Encyclopedia. McGraw-Hill Book Co., New York, 1965.

(20) Ölçer, Nurettin Y. On the Theory of Conductive Heat Transfer in Finite Regions with Boundary Conditions of the Second Kind. Int. J. Heat Mass Transfer 8:529-556, 1965.

(21) Olson, F.C.W. and J. M. Jackson. Heating Curves-Theory and Practical Application. Ind. Eng. Chem. 34-337-341, 1942.

(22) Olson, F.C.W. and O. T. Schultz. Temperatures in Solids During Heating or Cooling. Ind. Eng. Chem. 34:875-877, 1942.

(23) Perry, Russell L., F. M. Turrell and S. W. Austin. Thermal Diffusivity of Citrus Fruits. A paper from Heat Transfer, Thermodynamics and Education, edited by H. A. Johnson, pp. 242-246, McGraw-Hill Book Co., New York, 1964.

(24) Schneider, P. J. Conduction Heat Transfer. Addison-Wesley Pub. Co., Reading, Mass., 1955.

(25) Smith, R. E. and A. H. Bennett. Mass-Average Temperatures of Fruits and Vegetables during Transient Cooling. Trans. ASAE 8:249-252,1965.

(26) Thompson, G. E. Temperature-Time Relations in Canned Foods during Sterilization. Ind. Eng. Chem. 11: 657-664, 1919.

(27) Walters, Roger E. and K. N. May. Thermal Conductivity and Density of Chicken Breast, Muscle, and Skin. Food Technol. 17:130-133, 1963.

(28) Williamson, E. D. and L. H. Adams. Temperature Distribution in Solids During Heating or Cooling. Phys. Rev. 14:99-114, 1919.

VITA

Ralph Edward Smith

Candidate for the Degree of

Doctor of Philosophy

Thesis: ANALYSES ON TRANSIENT HEAT TRANSFER FROM ANOMALOUS SHAPES WITH HETEROGENEOUS PROPERTIES

Major Field: Engineering

Biographical:

Personal data: Born in Porterdale, Georgia, May 6, 1923, the son of James William Dennis and Flonnie Eliza Faulkner Smith.

Education: Attended Benedict grade school near Cedartown, Georgia; graduated with honor from Cedartown High School in 1941; received the degree of Bachelor of Science in Agricultural Engineering, cum laude, from the University of Georgia in June, 1948; received the Master of Science degree from the University of Georgia in June, 1961; completed the requirements for the Doctor of Philosophy degree from Oklahoma State University in May, 1966.

Professional experience: Taught agriculture in the Polk County Schools System, Cedartown, Georgia, 1948-53; taught physics and agricultural engineering at Abraham Baldwin Agricultural College, Tifton, Georgia, 1954-56; taught agricultural engineering and conducted research in the Agricultural Engineering Department of the University of Georgia, Athens, Georgia, 1956 to date.

Professional and honorary organizations: Member of the American Society of Agricultural Engineers, American Society for Engineering Education, Sigma Xi, Pi Mu Epsilon, Alpha Zeta, Phi Kappa Phi, Sigma Pi Sigma, and Sigma Tau. Registered Professional Engineer in Georgia.